BMC Plant Biology

RESEARCH

Open Access

PfERF106, a novel key transcription factor regulating the biosynthesis of floral terpenoids in *Primula forbesii* Franch

Xiancai Yin[1], Hongchen Yang[1], Keying Ding[1], Yuanzhi Luo[1], Wanqing Deng[1], Jianwei Liao[1], Yuanzhi Pan[1], Beibei Jiang[1], Xue Yong[1] and Yin Jia[1*]

Abstract

Background Flowers can be a source of essential oils used in the manufacture of substances with high economic value. The ethylene response factor (ERF) gene family plays a key role in regulating secondary metabolite biosynthesis in plants. However, until now, little has been known about the involvement of ERF transcription factors (TFs) in floral terpenoid biosynthesis.

Results In this study, an aromatic plant, *Primula forbesii* Franch., was used as research material to explore the key regulatory effects of *PfERF106* on the biosynthesis of terpenoids. *PfERF106*, which encodes an IXb group ERF transcription factor, exhibited a consistent expression trend in the flowers of *P. forbesii* and was transcriptionally induced by exogenous ethylene. Transient silencing of *PfERF106* in *P. forbesii* significantly decreased the relative contents of key floral terpenes, including (*z*)-β-ocimene, sabinene, β-pinene, γ-terpinene, linalool, eremophilene, α-ionone, and α-terpineol. In contrast, constitutive overexpression of *PfERF106* in transgenic tobacco significantly increased the relative contents of key floral terpenes, including *cis*-3-hexen-1-ol, linalool, caryophyllene, cembrene, and sclareol. RNA sequencing of petals of *PfERF106*-silenced plants and empty-vector control plants revealed 52,711 expressed unigenes and 9,060 differentially expressed genes (DEGs). KEGG annotation analysis revealed that the DEGs were enriched for involvement in secondary metabolic biosynthetic pathways, including monoterpene and diterpene synthesis. Notably, 10 downregulated DEGs were determined to be the downstream target genes of *PfERF106* affecting the biosynthesis of terpenoids in *P. forbesii*.

Conclusion This study characterized the key positive regulatory effects of *PfERF106* on the biosynthesis of terpenoids, indicating high-quality genetic resources for aroma improvement in *P. forbesii*. Thus, this study advances the artificial and precise directional regulation of metabolic engineering of aromatic substances.

Keywords *Primula forbesii*, Aromatic plant, Terpene metabolism, *ERF106*, RNA sequencing

Background

Plant aromatic ingredients are widely used in the cosmetic, light, and pharmaceutical industries to enhance the economic value of products. Floral fragrances are a complex mixture of volatile secondary metabolites with aromatic properties produced by plants. They play an important role in attracting pollinators as well as preventing natural enemies and the occurrence of diseases and pests [1, 2]. At present, more than 1700 floral

*Correspondence:
Yin Jia
jiayin_cn@163.com
[1] College of Landscape Architecture, Sichuan Agricultural University, Chengdu 611130, China

components have been identified. These components can be generally divided into three categories based on their biosynthetic pathways: terpenoids, aliphatic compounds and their derivatives, and benzenoids. Notably, the three categories have corresponding metabolic pathways [1, 3, 4]. Terpenoids are the largest group of volatile secondary metabolites and are produced by two biosynthesis pathways [5]. Components of the mevalonate (MVA) pathway are located in the cytosol, where they synthesize sesquiterpenoids and triterpenoids, and the 2-*C*-methyl-D-erythritol-4-phosphate (MEP) pathway, which occurs in the plastid and mainly synthesizes monoterpenoid and diterpenoid compounds [6–8]. Although these two metabolic pathways are isolated in subcellular space and the genes and enzymes in the pathways differ, the two pathways are related to each other and jointly participate in the biosynthesis of isopentenyl diphosphate (IPP), the precursor of terpenoids [9].

Transcription factors (TFs) uniquely exhibit "multipoint regulation," in which they simultaneously participate in regulating the expression of several key genes in a given metabolic pathway-related gene cluster, leading to the regulation of secondary metabolites. This phenomenon makes up for the insufficient action of a single key enzyme gene and instances in which multiple key enzyme genes may produce constitutive lethal expression, making manipulations of TFs an excellent tool for plant metabolic engineering [10]. In recent years, researchers have cloned and identified some TFs associated with the metabolism regulation of plant terpene floral compounds, such as bHLH [11, 12], WRKY [13], and bZIP [14]. Ethylene-responsive factors (ERF) are a subfamily of the APETALA2/ethylene-responsive factor (AP2/ERF) superfamily of plant-specific transcription factors. The AP2/ERF superfamily is mainly divided into four subfamilies: DREB (dehydration reaction element binding), ERF (ethylene reaction element binding protein), AP2 (APETALA2), and RAV (related to ABI3/VP). There are also a few unclassified factor Soloists subfamilies [15–20]. The ERF transcription factor family is widespread and abundant in plants. It plays an important role in regulating plant growth and development [21]. In addition, ERF transcription factors regulate the biosynthesis of volatile secondary metabolites in plants. For example, maize (*Zea mays* L.) *EREB58* promotes the expression of *TPS10* by directly binding to the GCC-box of the *TPS10* promoter, thus regulating sesquiterpene biosynthesis in leaves [22]. *CitERF71* regulates the biosynthesis of geraniol in sweet oranges (*Citrus sinensis* L.) [23]. In fragrant ornamental plants, such as petunia (*Petunia hybrida* Hook.), exogenous ethylene upregulates the *PhERF6* transcription factor, thereby affecting the expression of *ODO1* and several floral-related genes [24]. *ERF61* in osmanthus (*Osmanthus fragrans* Lour.) flower binds to the *CCD4* promoter and stimulates *CCD4* expression, thereby regulating the synthesis of β-ionone in petals [25]. In *Phalaenopsis bellina* Rchb.f. (Orchidaceae), *PbERF1* regulates the biosynthesis of monoterpenoids in flowers [26].

Primula forbesii Franch., in the family Primulaceae, like most members of its genus, blooms for 3–4 months, beginning in early spring, and has a strong floral scent [27], which can be used as an ideal material for extracting essential oils. Previous studies have posited that there are 10 terpenes, 21 phenylpropane compounds, and 38 fatty acid derivatives among the floral components of *P. forbesii*. Linalool, β-ocimene, α-terpineol, and other terpenes are the key floral components of *P. forbesii*, and the change trend of them increases first and then decreases during the flower opening, which gives *P. forbesii* a unique pleasant aroma [28]. Jia et al. used RNA sequencing to reveal vital gene information regarding the biosynthesis pathway of floral terpenes during *P. forbesii* floral development, laying an important foundation for understanding the floral metabolism mechanisms of *Primula* [29]. However, the transcriptional regulation of the metabolism of floral substances in *P. forbesii* remains unclear, and the regulatory effects of ERF transcription factors on the synthesis of floral substances in *P. forbesii* have not yet been reported.

In this study, a novel ethylene response factor, which was differentially expressed and consistent with the trend in floral terpenoid content in *P. forbesii*, was selected based on the transcriptome data from different flower development stages of *P. forbesii* [29]. The gene was cloned and named *PfERF106*, and it was preliminarily identified as being related to the synthesis of floral terpenes. Further research showed that *PfERF106* belongs to the IXb group of the ERF family and responds to induction by exogenous ethylene. Bidirectional verification tests of transient silenced homologously and heterologous overexpression revealed that *PfERF106* positively regulates the biosynthesis of floral terpenoid compounds. Transcriptome sequencing revealed the specific pathways and important target genes of *PfERF106* in regulating the metabolism and synthesis of terpenoids. This study provided an empirical basis for the genetic improvement of floral characters of *P. forbesii*.

Results

Sequence analysis of *PfERF106*

Herein, an AP2/ERF transcription factor exhibiting consistent expression during floral bloom was identified and named *PfERF106* (GenBank: PP436709) after cloning analysis based on the transcriptome data of four flowering stages of *P. forbesii* (Fig. 1). The open reading frame (ORF) of the *PfERF106* gene was determined to be 612

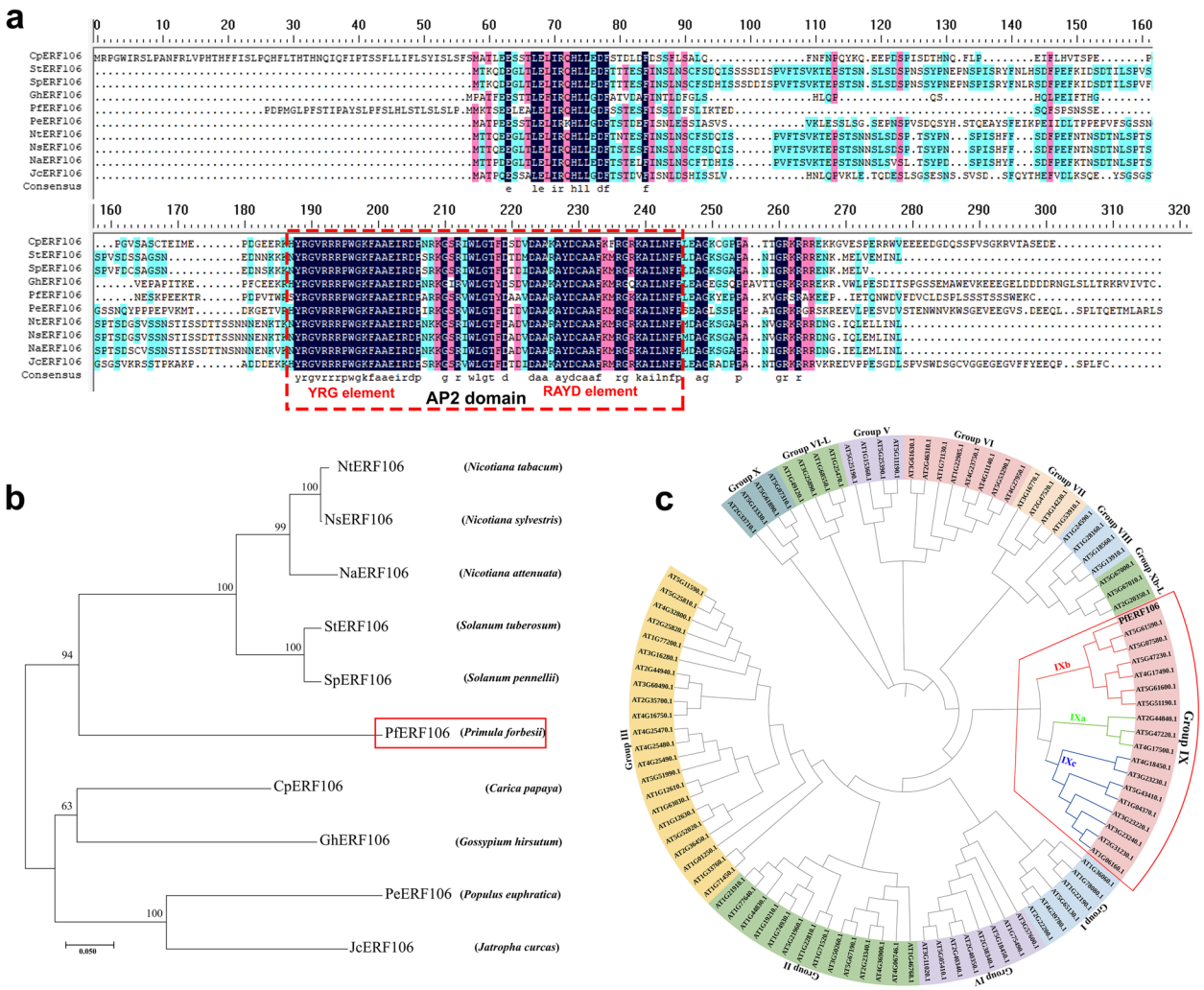

Fig. 1 Gene sequence analysis. **a** ERF106 homologous protein sequence alignment. **b** Phylogenetic tree of the PfERF106 protein. The accession umbers for these sequences are as follows (CpERF106, XP_021905462.1; StERF106, XP_006365343.1; SpERF106, XP_015074942.1; GhERF106, XP_016744472.1; PeERF106, XP_011022363.1; NtERF106, XP_016481253.1; NsERF106, XP_009771892.1; NaERF106, XP_019257925.1; JcRERF106, XP_012090504.1; PfERF106, WWS35502.1). **c** Comparison of the PfERF106 protein with ERF family proteins of *Arabidopsis thaliana* L

bp long and encode 203 amino acids (Supplementary Fig. 1a, b). Amino acid sequence analysis revealed that the *PfERF106* gene belongs to a large family of AP2/ERF transcription factors and has an AP2/ERF conserved domain. Notably, the 14th and 19th amino acids of the domain were determined to be alanine and aspartic acid, respectively, which provided additional evidence that *PfERF106* is indeed a member of the ERF subfamily of AP2/ERF transcription factors (Supplementary Fig. 1c). Further, the nuclear localization signal prediction tool NLStradamus was used to predict the nuclear localization signal in PfERF106 protein, and the prediction cutoff was set as 0.5. The amino acid sequence "GVRRRPWGKFAAEIR" at positions 99 to 113 of the PfERF106 protein was identified as the nuclear localization signal (Supplementary Fig. 1b). Protein homology retrieval and multiple sequence alignment revealed that ERF106 proteins in many plants have an AP2 domain (including YRG and RAYD elements) shared by the ERF family (Fig. 1a). Phylogenetic analysis revealed that PfERF106 is closely related to potato (*Solanum tuberosum* L.) StERF106 and tomato (*Solanum lycopersicum* L.) SpERF106 (Fig. 1b). By comparing the PfERF106 protein sequence with that of the ERF family protein sequence of *A. thaliana*, it was found that the *PfERF106* gene belongs to group IXb of the ERF subfamily (Fig. 1c).

Expression profile of *PfERF106* in *P. forbesii*

The spatiotemporal expression pattern of *PfERF106* and its response to ethylene induction were determined

(Fig. 2). *PfERF106* was expressed in four tissues, namely flowers (full flowering stage), leaves, stems and roots, with the highest expression in leaves, followed by roots and stems (Fig. 2a). The quantitative real-time PCR (qRT-PCR) results revealed that the relative expression level of *PfERF106* in the floral organs at the four flowering stages of *P. forbesii* first increased and then decreased (Fig. 2b). To investigate whether *PfERF106* can respond to ethylene induction, this study measured the expression of *PfERF106* after ethylene treatment at different concentrations and for different times. The exogenous ethylene treatment test showed that the relative expression of *PfERF106* was significantly increased by an ethylene concentration of 10 μL/L (Fig. 2c). Therefore, the petals were subsequently treated with 10 μL/L of ethylene for 0, 2, 4, 8, 12, and 24 h. *PfERF106* expression reached its peak after 4 h (Fig. 2d).

Confocal observation of *PfERF106* subcellular localization

In order to analyze the subcellular localization of PfERF106, the plasmid p131-ERF106-YFP was transformed into *Agrobacterium* GV3101 by the liquid nitrogen freeze-melt method in this study. *Agrobacterium* was cultured overnight, centrifuged, and then resuspended (10 mmol/L $MgCl_2$, 10 mmol/L MES, and 100 μmol/L Acetosyringone). After standing at room temperature for 3 h, suitable leaves of *N. benthamiana* were selected for injection, and confocal observation was performed after

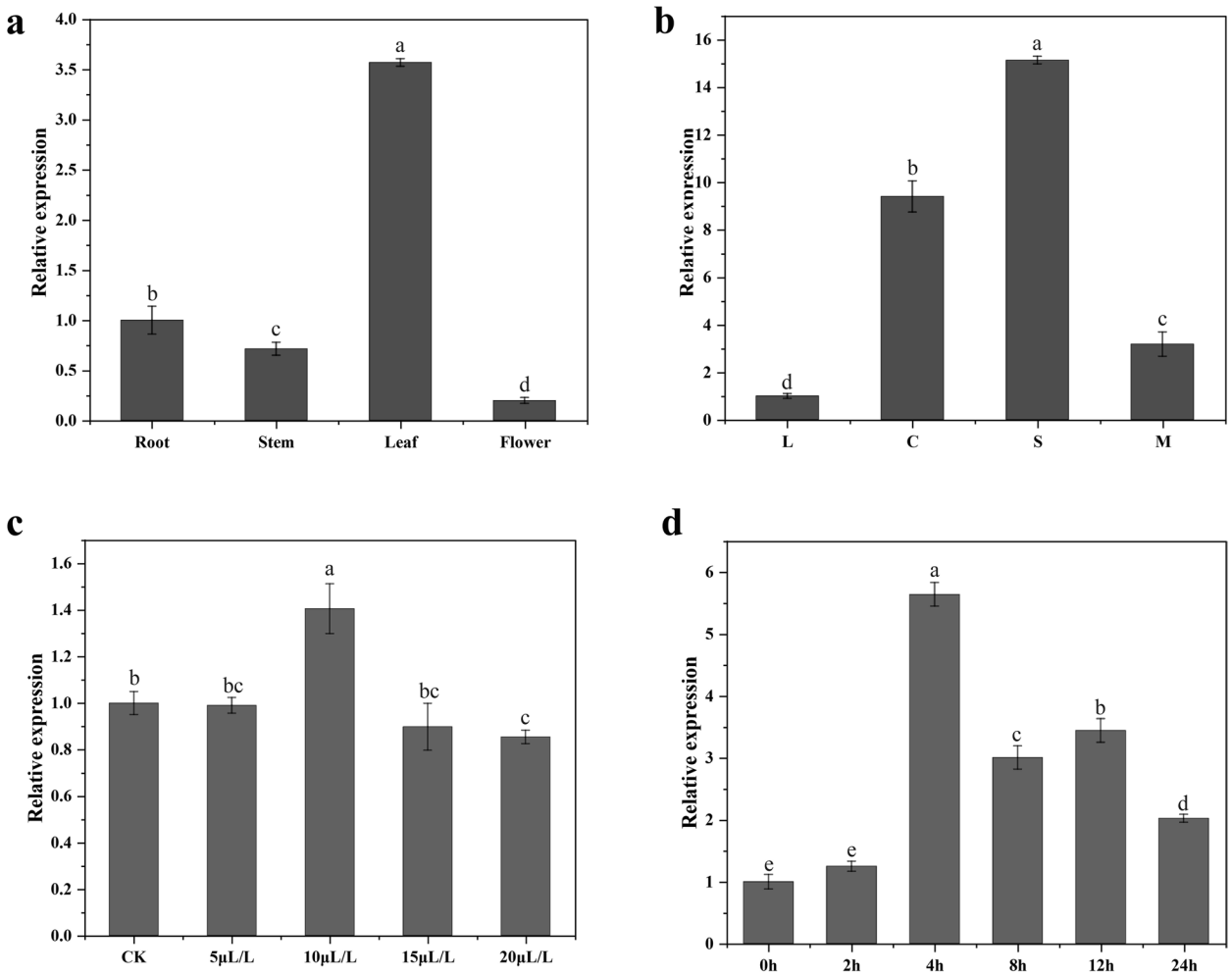

Fig. 2 Spatiotemporal expression and response hormone of *PfERF106*. **a** Expression of *PfERF106* in different tissues of *P. forbesii* (flowers in full flowering stage; leaves; stems; roots). **b** Expression of *PfERF106* at different flowering stages of *P. forbesii* (L, Petals of the bud stage; C, first flowering stage; S, full flowering stage; M, late flowering stage). **c** *PfERF106* response to ethylene treatment at varying concentrations. **d** *PfERF106* response to 10 μL/L of ethylene treatment at varying timepoints. All the images were drawn using Origin 2021, and SPSS 28.0 was used for data analysis. Data are expressed as mean ± SD of three replicates. Treatments labelled with different lowercase letters were significantly different at a threshold of $p < 0.05$

3 d injection. As can be seen from Fig. 3, the fusion protein of PfERF106-YFP was localized to the nucleus.

Transient silencing of *PfERF106* significantly inhibited terpenoid synthesis in *P. forbesii*

In this study, mixed infection culture consisting of TRV1 and TRV2-*PfERF106*, based on tobacco rattle virus (TRV), was injected into the back of the leaves of *P. forbesii*, and the phytoene desaturase (*PDS*) gene was used as a marker gene to verify the effectiveness of the system. Notably, new leaves of TRV2-*PfPDS*-infected plants showed obvious chlorosis; the stems changed from green to white, and the petals exhibited significant faintness of pigmentation at 6 weeks post-injection. TRV2-*PfERF106*- and TRV2-infected plants grew normally; the leaves and stems were a typical dark green, and the petals were pink-purple (Fig. 4a). Four *PfERF106*-silencing positive transgenic lines, 106-1, 106-2, 106-3, and 106-5, were identified by agarose gel electrophoresis. Notably, the silencing effect in the three *PfERF106*-silenced lines 106-1, 106-2, and 106-3 was better (Fig. 4b), exhibiting relative expression levels of 0.17, 0.25, and 0.24 times that of the control line, respectively.

The gas chromatography-mass spectrometry (GC-MS) results indicated that the peak height of key terpenes between the control and treatment group was significantly different; the treatment group exhibited a decreasing trend compared to the control group (Fig. 4c). Further analysis of the relative contents of key floral terpenes revealed a significant decrease in the relative contents of (*z*)-β-ocimene, sabinene, β-pinene, γ-terpinene, linalool, eremophilene, α-ionone, and α-terpineol in gene-silenced plants compared to control plants (Fig. 4d). The relative contents of sabinene, eremophilene, α-ionone, α-terpineol, and β-pinene were 0.11, 0.04, 0.04, 0.11, and 0.20 times those of the control group, and those of (*z*)-β-ocimene and γ-terpinene were 0.49 and 0.67 times those of the control group, respectively. The content of linalool, a key floral substance in *P. forbesii*, in the gene-silenced plants was significantly lower than that in the control group.

Additionally, qRT-PCR results revealed that the relative expression levels of *PfLIS* (encoding linalool synthase)

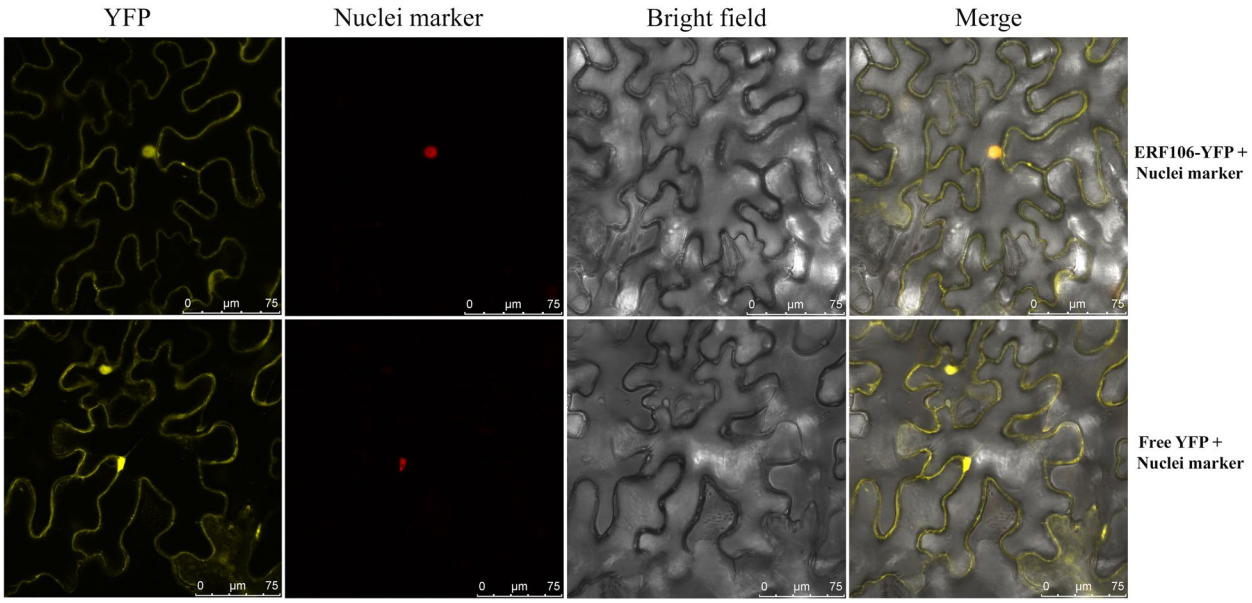

Fig. 3 Subcellular localization of PfERF106. Fluorescence signals were visualized using a confocal laser scanning microscope. Yellow fluorescence indicated yellow fluorescent protein (YFP). Red fluorescence indicated nuclei marker fluorescence

(See figure on next page.)

Fig. 4 Transient silencing of *PfERF106* in *P. forbesii*. **a** Phenotypes of the whole plant, flowers, stems, and leaves after the transient silencing of *PfERF106* in *P. forbesii*. **b** Detection of the relative expression of *PfERF106* in different lines. **c** The floral contents of *PfERF106*-silenced plants were detected by GC-MS. The variation in floral content was visually demonstrated by using the empty vector plant and the line with the highest gene silencing ratio (i.e., 106-1). **d** Relative contents of key terpenoids in flowers of control and silenced plants. The silenced lines with three similar levels of silencing (106-1, 106-2, 106-3) were treated as three biological replicates. **e** Expression of key genes associated with the biosynthesis of floral terpenes. Data are expressed as means ± standard deviations of three replicates (***, $p < 0.001$; **, $p < 0.01$; *, $p < 0.05$)

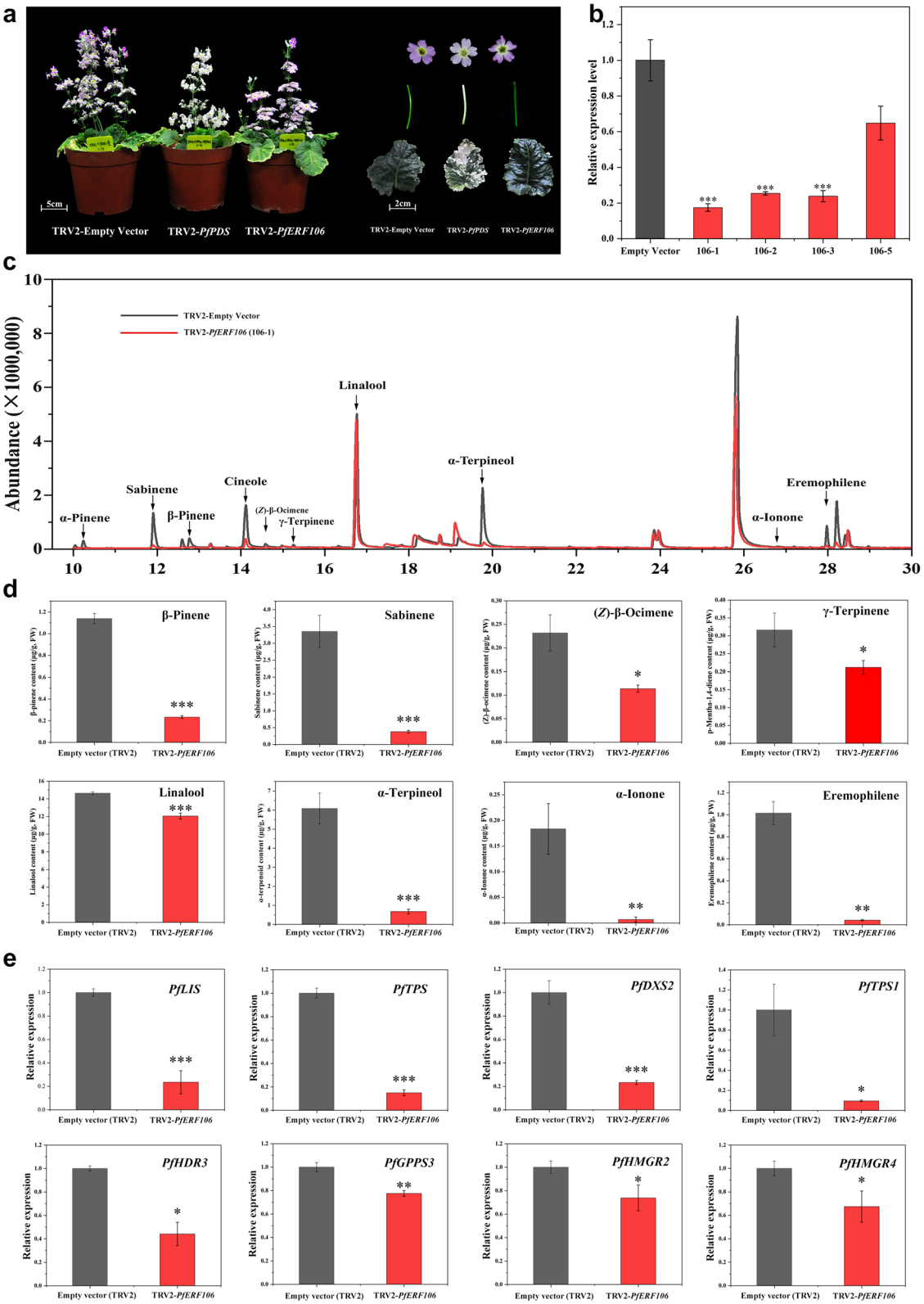

Fig. 4 (See legend on previous page.)

and *PfTPS* (encoding α-terpineol synthase) in *PfERF106*-silenced plants were significantly lower than the corresponding levels in the control group, i.e., by 0.24 and 0.15 times, respectively. Moreover, an analysis of the relative expression of key genes involved in the terpene metabolic pathway of *P. forbesii* revealed significant downregulation of *PfDXS2*, *PfTPS1*, *PfHDR3*, *PfGPPS3*, *PfHMGR2*, and *PfHMGR4* in the MEP and MVA pathways relative to the control group. The relative contents of the genes were 0.23, 0.10, 0.44, 0.78, 0.74, and 0.67 times those of the control, respectively (Fig. 4e).

Constitutive overexpression of *PfERF106* promoted terpenoid biosynthesis in tobacco

Seven transgenic *PfERF106* overexpression (OE) lines, OE-2, OE-3, OE-12, OE-13, OE-14, OE-16, and OE-19, were selected to study the effect of stable overexpression of *PfERF106* on terpenoid biosynthesis in tobacco. The expression of *PfERF106* in these strains was significantly higher than that of the wild type, reaching 22.08, 77.78, 21.05, 61.01, 247.13, 18.76, and 31.55 times that of the wild type, respectively (Fig. 5a). Wild-type plants with healthy growth and two OE transgenic lines with high expression levels of *PfERF106* were selected for subsequent experiments. Plant phenotype observations revealed that the OE-14 line, which had the highest *PfERF106* expression level, flowered first, while the OE-13 line flowered slightly later. Notably, both lines flowered earlier than wild-type tobacco (Fig. 5b).

GC-MS results revealed that the peak height of key terpenes in OE transgenic tobacco was significantly different from that of wild-type tobacco. Moreover, there was an increasing trend in the treatment group compared to the control group (Fig. 5c). The relative contents of key terpene substances, such as *cis*-3-hexen-1-ol, linalool, caryophyllene, cembrene, and sclareol, in OE transgenic tobacco petals were significantly increased compared to the control (Fig. 5d). An increase in the relative expression level of *PfERF106* significantly increased the relative contents of key terpene substances. Among them, the relative contents of *cis*-3-hexen-1-ol, caryophyllene, cembrene, and sclareol in OE-13 and OE-14 lines were 1.93 and 5.43 times, 4.84 and 18.23 times, 1.62 and 5.01 times, and 1.11 and 5.16 times those of the control, respectively. Notably, the change of linalool content in OE-13 and OE-14 strains was the most significant, reaching 13.68 and 35.75 times that of the control, respectively.

Prediction of downstream *PfERF106* gene targets

Data assembly and annotation

RNA-seq was used to establish a transcriptome database of *PfERF106*-silenced lines and empty-vector control lines of *P. forbesii*. The total number of transcripts obtained after screening was 114,690, while the total length of the sequences was 153,500,473 bp. The maximum transcript length was 16,868 bp. The N50 value (i.e., the length cutoff for the longest assembled sequences that contain 50% of the total transcriptome length) was 1,904 bp, and the total number of sequences longer than this was 26,124. Similarly, the N90 value was 609 bp, and the total number of longer sequences was 79,431. In addition, the average GC content of all sequences was 39.7%. A total of 52,711 unigenes were obtained after sequence assembly using Trinity (v2.15.1) software. The total sequence length of the unigenes was 60,150,613 bp, with a maximum sequence length of 16,868 bp and an N50 of 1,772 bp. The total number of sequences with a length greater than N50 and N90 were 10,568 and 36,819, respectively. In addition, the average GC content of all the obtained unigene sequences was 39.11% (Table 1).

NR, GO, KEGG, Pfam, eggNOG, and Swiss-Prot databases were used to annotate the functions of the unigenes (Table 2). Notably, 25,960 unigenes were successfully annotated using the NR database, accounting for 49.25% of the total number of unigenes. The unigenes successfully annotated using the GO, KEGG, Pfam, eggNOG, and Swiss-Prot databases were 15,782, 8,566, 16,856, 24,626, and 20,182, accounting for 29.94%, 16.25%, 31.98%, 46.72%, and 38.29% of the total number of the unigenes, respectively. The number of unigenes successfully annotated using every one of the databases was 5,289, accounting for 10.03% of the total number of unigenes.

The similarities between the gene sequences of *P. forbesii* and those of related species as well as the functional annotation of *P. forbesii* genes were obtained by comparing and annotating them using the NR database (Fig. 6a). The E-value distribution map showed that 53.95% of the annotated sequences had strong homology ($0 < \text{E-value} < 10^{-45}$). The most unigene sequences were most similar to tea (*Camellia sinensis* L.), followed by *Actinidia chinensis* var. *chinensis*, *Actinidia rufa* Planch., *Nyssa sinensis* Oliver., and *Rhododendron griersonianum* Balf. f. et Forrest, *Rhododendron simsii* Planch., and *Vitis vinifera* L., in that order, accounting for 26.22%, 14.44%, 5.23%, 4.99%, 3.96%, 3.66%, and 2.19% of unigenes, respectively. The number of genes annotated for their biological process, cellular component, and molecular function in the GO database were 53,989, 17,846, and 24,397, accounting for 56.10%, 18.54%, and 25.35% of unigenes, respectively (Fig. 6b). The top five KEGG functions were metabolism, genetic information processing, environmental information processing, cellular processes, and organismal systems (Fig. 6c). Notably, the metabolism (based on KEGG annotation) of terpenoids and polyketides and biosynthesis of other secondary

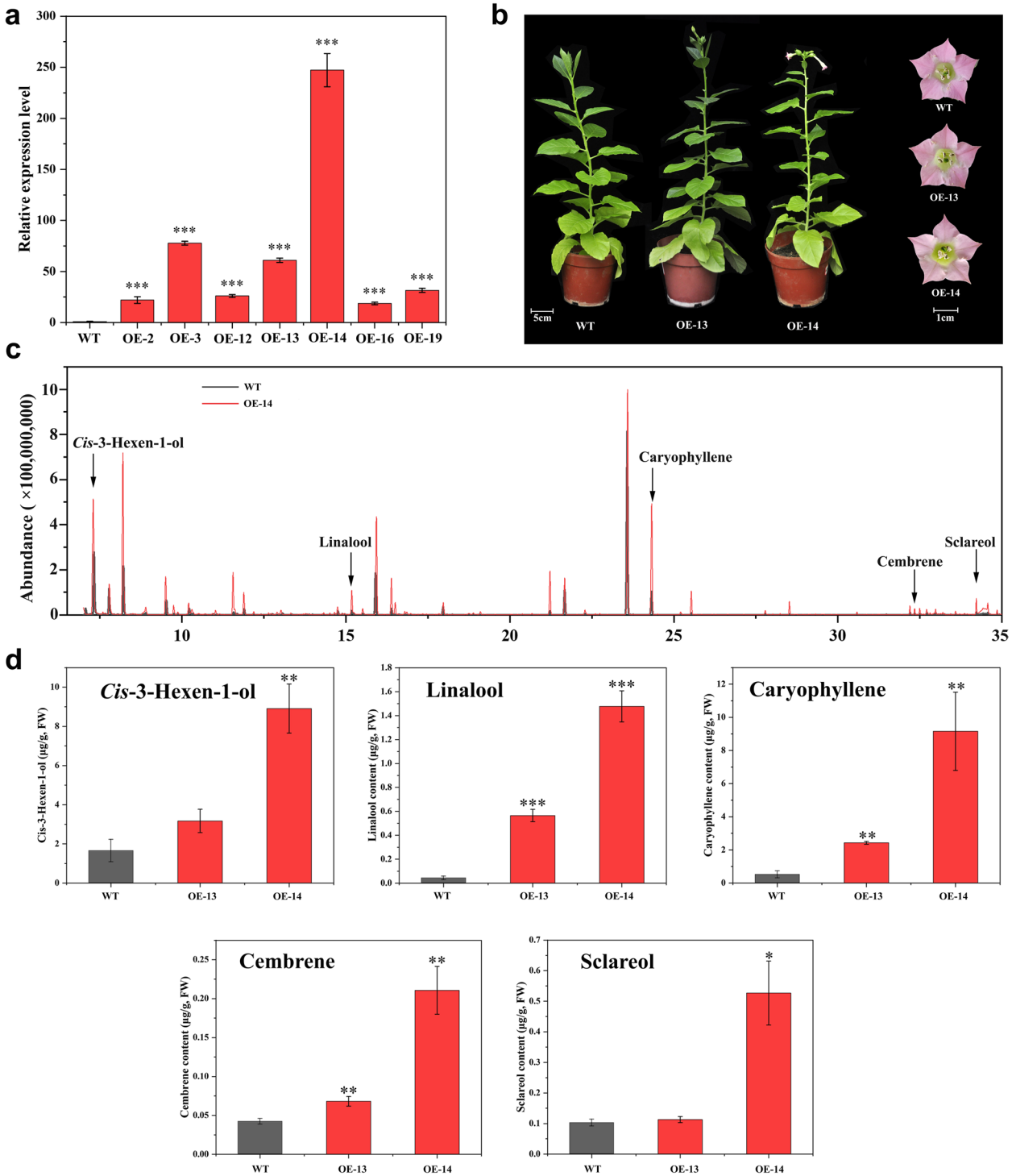

Fig. 5 Constitutive overexpression of *PfERF106* in tobacco (WT, wild type; OE, overexpression). **a** Detection of the relative expression of *PfERF106* in different lines. **b** Phenotypes of the whole plant and flowers after constitutive overexpression of *PfERF106* in tobacco. **c** The floral content of *PfERF106*-overexpression plants was detected by gas chromatography-mass spectrometry. The variation in floral content was visually demonstrated by using the wild-type plant and the line with the highest gene overexpression ratio (OE-14). **d** Relative contents of key terpenoids in flowers of control and overexpression plants

Table 1 Assembly results of *P. forbesii* transcriptome

Contig	Transcript	Unigene
Total Length (bp)	153,500,473	60,150,613
Sequence Number	114,690	52,711
Max. Length (bp)	16,868	16,868
N50 (bp)[a]	1,904	1,772
N50 Sequence No.[b]	26,124	10,568
N90 (bp)[c]	609	475
N90 Sequence No.[d]	79,431	36,819
GC%[e]	39.77	39.11

[a] N50 (bp) : Arrange all sequences from long to short, add the length of the sequence in that order, and when the length of the addition reaches 50% of the total length of the sequence, the length of the last sequence

[b] N50 Sequence No. : The total number of sequences whose length is greater than N50

[c] N90 (bp) : All sequences are arranged by length from longest to shortest, and the length of the sequence is added in this order. When the length of the addition reaches 90% of the total length of the sequence, the length of the last sequence

[d] N90 Sequence No. : The total number of sequences longer than N90

[e] GC% : The GC content of the sequence

Table 2 Unigene functional annotation results among different databases

Database	Number	Percentage
NR	25,960	49.25
GO	15,782	29.94
KEGG	8,566	16.25
Pfam	16,856	31.98
eggNOG	24,626	46.72
Swissprot	20,182	38.29
In all database	5,289	10.03

metabolites corresponded to 160 and 237 functional annotation results, respectively. The eggNOG database was used to annotate 2,113 unigenes as signal transduction mechanisms and 2,087 unigenes as associated with posttranslational modification, protein turnover, and chaperones. Notably, 880 unigenes were classified as involved in secondary metabolite biosynthesis, transport, and catabolism (Fig. 6d).

Principal component analysis and correlation analysis revealed a strong correlation between the performance of samples in silenced (M) and control plants (CK). Notably, there was high similarity in the expression patterns among the samples (Fig. 6e, f). In this study, after transcriptome sequencing of *PfERF106*-silenced lines and empty-vector control lines of *P. forbesii*, a large number of genes related to terpene synthesis were obtained by KEGG annotation analysis. To verify the reliability of transcriptome data after *PfERF106*-silencing, 12 differentially expressed genes, especially those related to terpenoid metabolism, were randomly selected for quantification to verify the reliability of gene expression estimates based on RNA-Seq. Notably, the qRT-PCR data for these genes was highly consistent with the fragments per kilobase of transcript per million mapped reads (FPKM) values of the RNA-seq transcriptome data (Fig. 7a). Linear regression analysis revealed a correlation of 87.58% between RNA-seq and qRT-PCR data (Fig. 7b), indicating that the transcriptome data were indeed reliable.

Analysis of genes associated with differential gene expression and terpenoid synthesis

Differential gene expression analysis identified 9,060 differentially expressed genes (DEGs): 4,534 upregulated and 4,526 downregulated genes. GO enrichment analysis of DEGs showed that secondary metabolite synthesis processes were enriched in the first 10 GO term entries among biological processes (Fig. 8a). The metabolism pathway was the most enriched KEGG pathway among the 30 pathways and had the lowest *p*-value. There were two types of metabolic pathways identified: diterpenoid biosynthesis and monoterpenoid biosynthesis (Fig. 8b). Notably, the top 20 KEGG pathways with the lowest false discovery rate (FDR) value had these two types of metabolic pathways (Fig. 8c). These biological processes are potentially vital to the synthesis of terpenoid floral compounds. In addition, a total of 1,236 transcription factors were differentially expressed in this study (Fig. 8d) including 60, 37, and 21 downregulated members of the ERF, bHLH, and MYB transcription factor families, respectively.

Changes in the DEGs associated with terpenoid synthesis associated with *PfERF106* silencing were further analyzed utilizing the transcriptome data to explore the regulatory effect of *PfERF106* on the synthesis of floral terpenoids in *P. forbesii* (Table 3). Notably, 60 DEGs were annotated as participating in the synthesis of terpenoids. Among them, seven were associated with diterpenoid biosynthesis, while three were associated with monoterpenoid biosynthesis. Similarly, there were three DEGs, nine DEGs, another nine DEGs, and one DEG associated with sesquiterpenoid and triterpenoid biosynthesis, ubiquinone and other terpenoid-quinone biosynthesis, terpenoid backbone biosynthesis, and limonene and pinene degradation, respectively. In addition, there were 7, 13, and 8 DEGs associated with the terpenoid and polyketones metabolic pathways, including brassinosteroid biosynthesis, carotenoid biosynthesis, and zeatin synthesis, respectively. The DEGs were classified into MEP and MVA metabolic pathways based on the annotation information and metabolic pathways. One unigene was predicted to encode *DXS* in the MEP pathway, while

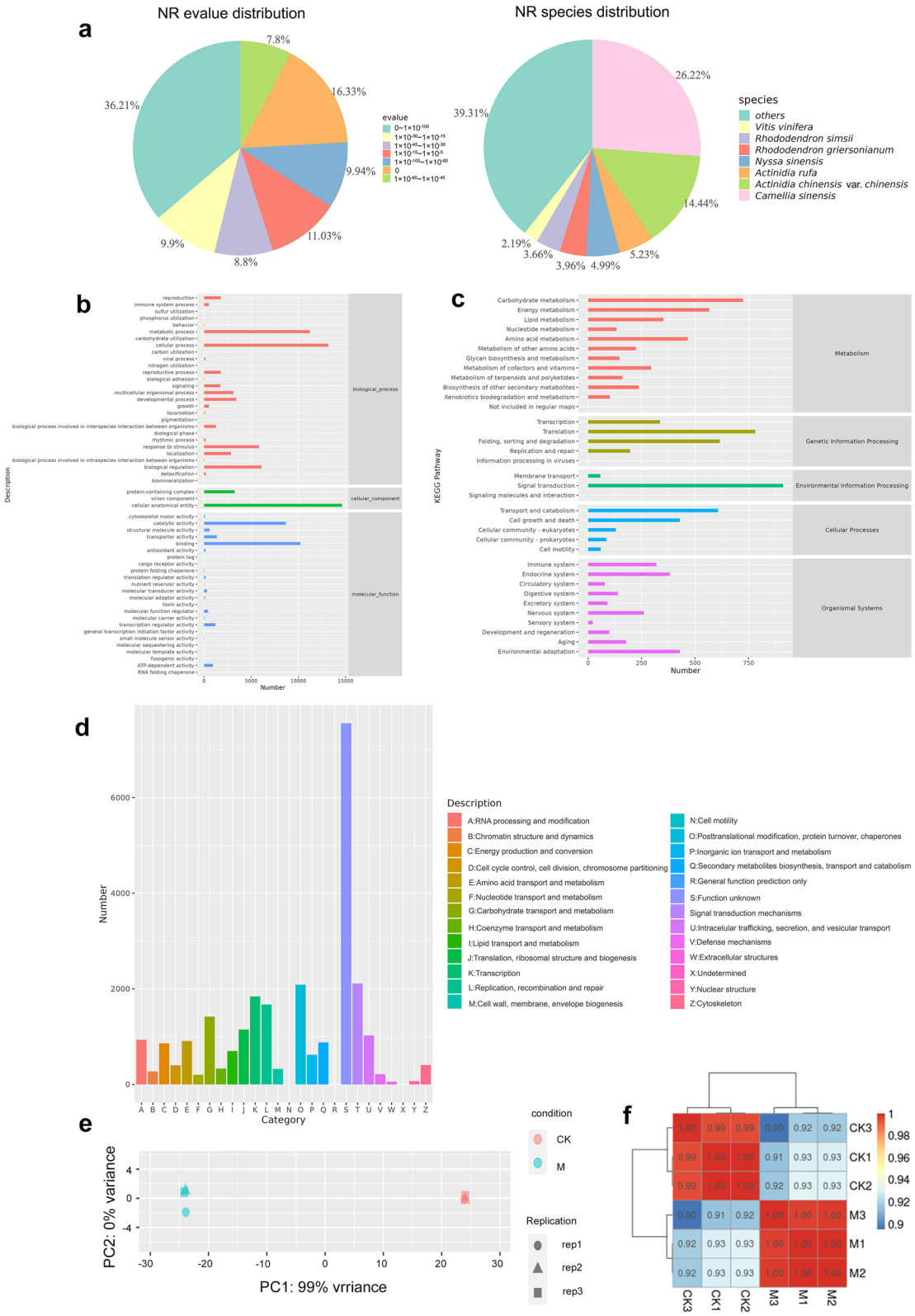

Fig. 6 Annotation of the unigene functions according to different databases. **a** E-value and species distribution of the top BLAST hits for each unique sequence. **b** The annotation results of the GO database. **c** The annotation results of the KEGG database. **d** The annotation results of the eggNOG database. **e** A principal component analysis of the gene expression level. **f** Correlation analysis of the samples. GO, Gene Ontology; KEGG, Kyoto Encyclopedia of Genes and Genomes

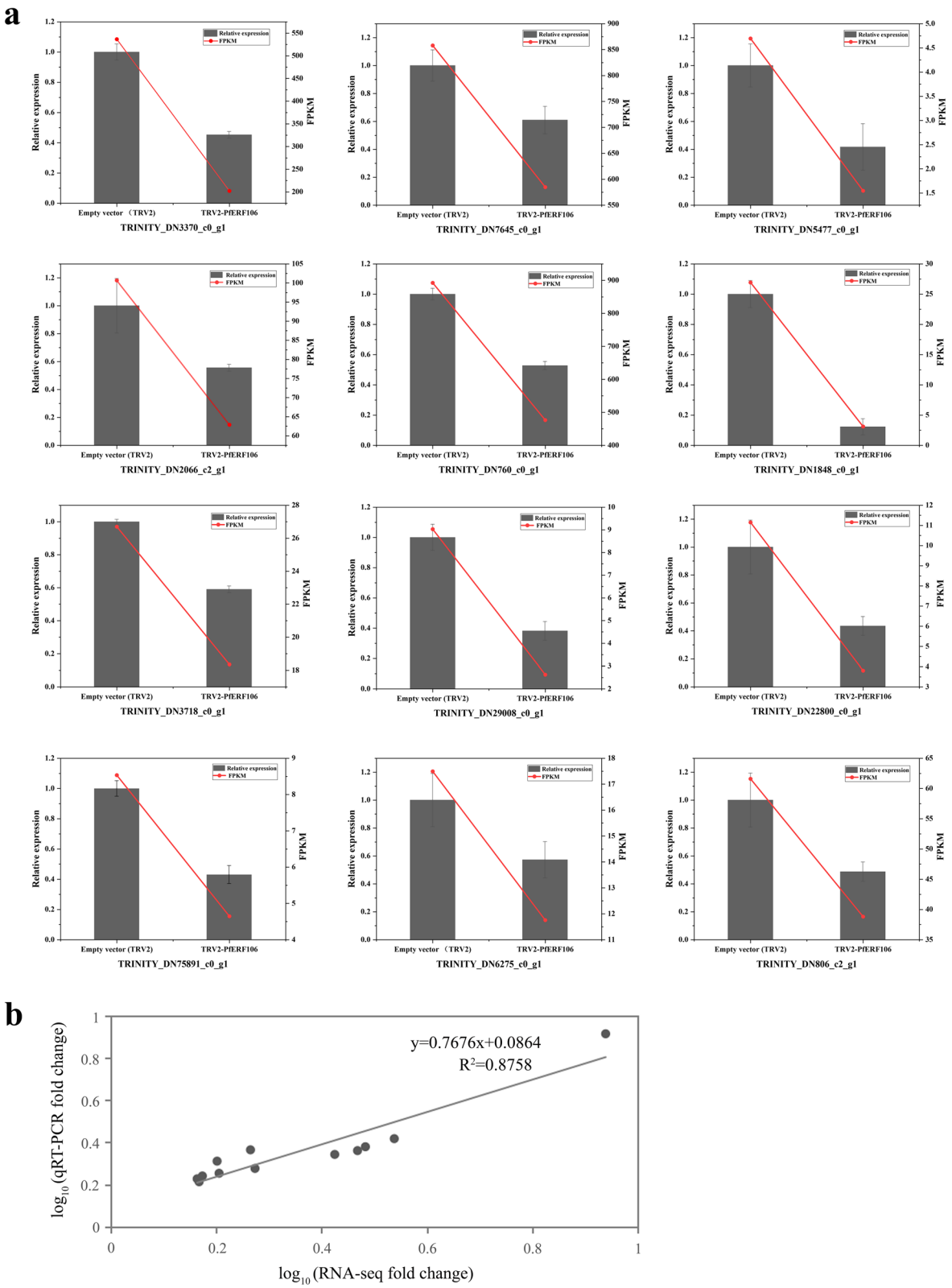

Fig. 7 The qRT-PCR validation of 12 differentially expressed genes (DEGs). **a** The qRT-PCR analysis of 12 terpene biosynthesis-associated genes. The bar chart shows the relative gene expression based on qRT-PCR (left *y*-axis), while the line chart shows the fragments per kilobase of transcript per million mapped reads (FPKM) value of RNA-Seq (right *y*-axis). The error bar represents the standard deviation of three independent replicates. **b** Correlation analysis of fold-change values obtained from RNA-seq and qRT-PCR analyses. qRT-PCR, real-time quantitative reverse transcription PCR

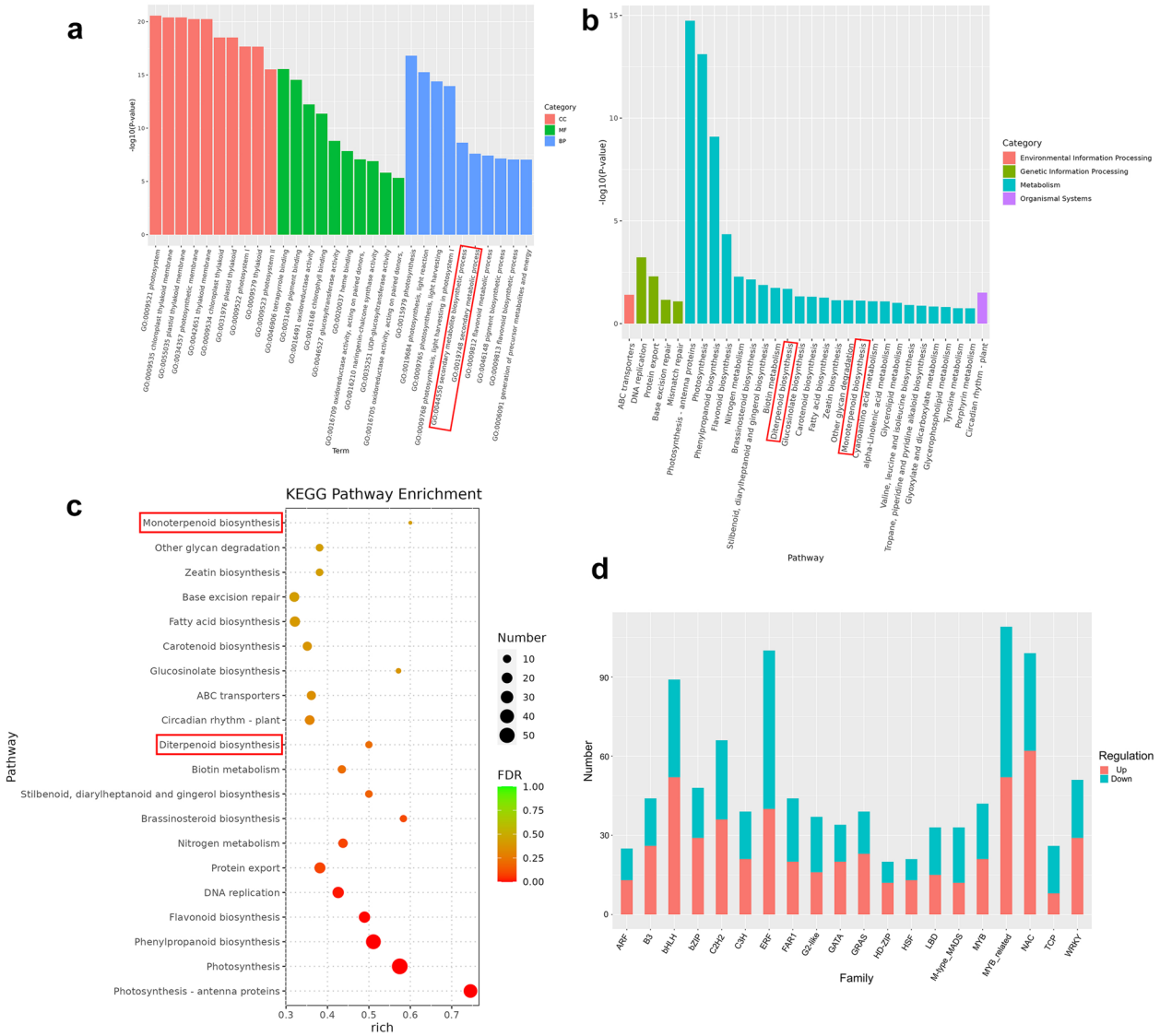

Fig. 8 Analysis of the differentially expressed genes (DEGs). **a** The top 10 GO terms with the lowest *p*-value in each GO classification in the GO enrichment analysis of DEGs. **b** The top 30 pathways with the lowest *p*-value in KEGG annotation results of DEGs. **c** The top 20 pathways with the lowest false discovery rate (FDR) in the KEGG annotation results of DEGs. **d** Statistics of the differential expression of transcription factors. GO, Gene Ontology; KEGG, Kyoto Encyclopedia of Genes and Genomes

the other unigenes were predicted to encode 4-hydroxy-3-methylbut 2-enyl diphosphate reductase (*HDR*), geranyl diphosphate synthase (*GDPS*), and nerolidol synthase (*NES*). In the MVA pathway, one unigene was predicted to participate in the expression of hydroxymethylglutaryl-CoA reductase (*HMGR*) and acetyl-CoA C-acetyltransferase (*AACT*) (Table 4).

Discussion

PfERF106 is a potential regulator of terpenoid metabolism

Plants produce special metabolites with diverse structures, such as alkaloids and terpenes, in response to biological and abiotic environmental stresses. This process is dynamically regulated by metabolic genes associated with specific pathways and usually occurs at the transcription level, mediated by transcription factors (TFs) [30–32]. TFs coordinate the transcription of multiple metabolic pathways and affect gene expression within the same metabolic pathway [33–35]. Studies have postulated that AP2/ERF is widely involved in plant biological processes and plays a vital role in regulating the biosynthesis of primary and secondary metabolites of plants, including *Catharanthus roseus* L [36]. and *Artemisia annua* L [37]. These previous results indicate that

Table 3 Annotation analysis and quantitative statistics of differentially expressed genes related to floral terpenoid synthesis in *P. forbesii*

KO number	Pathway	Number of DEGs	Upward number	Down number
ko00904	Diterpenoid biosynthesis	7	4	3
ko00902	Monoterpenoid biosynthesis	3	0	3
ko00909	Sesquiterpenoid and triterpenoid biosynthesis	3	2	1
ko00130	Ubiquinone and other terpenoid-quinone biosynthesis	9	3	6
ko00900	Terpenoid backbone biosynthesis	9	4	5
ko00903	Limonene and pinene degradation	1	1	0
ko00905	Brassinosteroid biosynthesis	7	2	5
ko00906	Carotenoid biosynthesis	13	5	8
ko00908	Zeatin biosynthesis	8	6	2

Table 4 Key downregulated genes of floral terpenoids involved in biosynthesis in *P. forbesii*

Gene name	Annotation	KO Number	Pathway	Unigene
DXS2	1-deoxy-D-xylulose-5-phosphate synthase	ko00900	MEP	TRINITY_DN7645_c0_g1
HDR	4-hydroxy-3-methylbut-2-enyl diphosphate reductase	ko00900	MEP	TRINITY_DN7265_c0_g1
GDPS	Geranyl diphosphate synthase	ko00900	MEP	TRINITY_DN27786_c0_g1
HMGR	hydroxymethylglutaryl-CoA reductase	ko00900	MVA	TRINITY_DN24032_c0_g2
AACT	acetyl-CoA C-acetyltransferase	ko00900	MVA	TRINITY_DN6960_c0_g1
MNR	neomenthol dehydrogenase	ko00902	MEP	TRINITY_DN30937_c0_g1
SDR	Short-chain dehydrogenase/reductase	ko00902	MEP	TRINITY_DN6275_c0_g1
NES	(3 S,6E)-nerolidol synthase	ko00902	MEP	TRINITY_DN3370_c0_g1
SM	Squalene monooxygenase	ko00909	MVA	TRINITY_DN696_c0_g1
KS	Ent-kaurene oxidase	ko00904	MEP	TRINITY_DN922_c1_g4

PfERF106, a member of the AP2/ERF transcription factor family, is highly likely to participate in the biosynthesis of plant secondary metabolites. Nakano et al. divided the ERF family genes of *A. thaliana* into 12 groups, Group I to Group X, Group VI-L, and Group Xb-L, based on their gene structure and conserved motifs [17]. Further analysis revealed that genes in Group IX of the ERF family are typically involved in the expression of defense genes in response to pathogen infection. For example, overexpression of *ERF1* in *A. thaliana* and of *Pti4* in tomato (*S. lycopersicum*) has been shown to enhance resistance to necrotic fungi, bacteria, and biotrophic fungi [38, 39]. In addition, relevant studies have postulated that genes in this group participate in the control of secondary metabolite synthesis by interacting with the GCC-box region in the promoter [40]. For example, *Litsea cubeba* Lour. *LcERF19*, a member of the IXb group of the ERF family, positively regulates the production of geranial and neral by binding to the *LcTPS42* promoter [41]. The transcription factor *CitERF71* of sweet orange (*C. sinensis*) belongs to Group IXa of the ERF gene family and activates the terpene synthase gene involved in (*E*)-geraniol synthesis [23]. These reports strongly suggest that *PfERF106*, a member of the IXb group of the ERF family, is highly likely to participate in the biosynthesis of floral volatiles, especially terpenes.

In this study, *PfERF106* was highly expressed in the roots and leaves but expressed at a low level in stems and flowers, consistent with the observed trend of the transcription factor *LcERF19*, which is associated with the metabolism of geranial and neral [41]. Similarly, *PhERF6* is associated with floral biosynthesis in petunias (*P. hybrida*) and is highly expressed in the roots and stems but expressed at a low level in the corolla [24]. These reports suggest that gene function of homologous genes in different plants often exhibit different levels of expression in different tissues, as TFs have more diverse and complex regulatory roles than key functional genes in metabolic pathways and can bind to various suitable DNA contact sites and recruit other proteins for the regulation of different functions [42].

It has been posited that AP2/ERF transcription factor members, especially members of the ERF subfamily, are involved in growth, development, stress, and various

responses and can be induced by defense-related plant hormones, such as ethylene, jasmonic acid, and salicylic acid [43, 44]. For example, *PhERF* genes in petunias are highly expressed after 4 h and 8 h of treatment with exogenous ethylene [16]. Similarly, the present study showed that *PfERF106*, an ethylene response factor, can respond to exogenous ethylene treatment. Ethylene is a gaseous plant hormone involved in many physiological and biochemical reactions throughout the life processes of plants and is closely associated with the synthesis and release of plant aroma. It can affect the release of terpenoids and the expression and transcription levels of related genes in *Antirrhinum majus* L [45]. , *P. hybrida* [46, 47], and *Lathyrus odoratus* [48]. These results suggest that *PfERF106*, as a factor downstream of ethylene, may be involved in floral release in response to ethylene signals during flower development.

Transcription factors typically play a transcriptional regulatory function in the nucleus [49]. In this study, the protein encoded by *PfERF106* was located in the nucleus. In addition, some proteins encoded by terpene synthase genes are usually localized to chloroplasts or cytoplasm, such as S*tevia rebaudiana* SrTPS1-5, which can affect monoterpenoids or sesquiterpenoids biosynthesis [50]. These results suggest that *PfERF106* may be involved in the regulation of nuclear gene transcription, and then affect the expression of downstream genes such as terpene synthase genes in cytoplasm, thus affecting the biosynthesis of terpenoids.

PfERF106 positively regulated the biosynthesis of terpenoids

Virus-induced gene silencing (VIGS) is a technique that uses RNA-mediated antiviral immunity and can thus be utilized in all plants as a post-transcriptional gene silencing (PTGS) mechanism [51]. Gene silencing (TRV-VIGs) induced by tobacco rattle virus (TRV) has many advantages, such as its high silencing efficiency and long duration. It is widely used in various plants, including tomato (*S. lycopersicum*) [52], tobacco (*Nicotiana tabacum* L.) [53], and *P. hybrida* [54, 55].

In this study, TRV induced the silencing of *PfERF106* and reduced the relative content of floral terpenoids in plants. These results are similar to those of *O. fragrans OfERF61* [25] and *Z. mays EREB58* [22], which also regulate the synthesis of volatile terpenoids. Similarly, *SmERF128* [56] and *SmERF6* [57] from *Salvia miltiorrhiza* Bunge and *CsERF061* [58] from *C. sinensis* participate in the regulation of non-volatile terpenoid synthesis. These results strongly suggested that *PfERF106* is positively involved in regulating the synthesis of terpene floral substances in *P. forbesii*.

Notably, this study found that the silencing of *PfERF106* significantly reduced linalool content and *PfLIS* gene expression. This finding is consistent with that of Wei et al. [59], who found that transient overexpression of *PpERF61* in peach (*Prunus persica* L.) fruit significantly increased linalool content and the expression levels of the linalool synthase genes *PpTPS1* and *PpTPS3*, suggesting that *PfERF106* affects the synthesis of linalool by upregulating the expression of the linalool synthase gene *PfLIS*. Although the content of linalool in the silenced strain was significantly lower than that in the control group, the decline factor was slightly lower, indicating that linalool, as the floral component with the largest relative content in *P. forbesii* [28], had an abundance of its substrate. The inhibited expression of a single transcription factor cannot completely block the synthesis of downstream secondary metabolites.

In addition, we found that the trend of gene expression in the terpenoid synthesis pathway was consistent with that of *PfERF106* expression. This finding is consistent with that of Wang et al. [41], who showed that transient overexpression of *LcERF19* in *C. chinensis* increased the expression levels of *LcDXS*, *LcHMGR*, and other terpenoid biosynthetic pathway genes. Similarly, transcriptomic sequencing conducted by Wan et al. [60] after treating *A. annua* with different forms of phosphorus revealed that several artemisinin biosynthesis genes, such as *DXS*, *GPPS*, and *GGPS*, were co-upregulated with 21 transcription factor family genes, including the ERF family. This finding suggested that ERF transcription factors are strongly correlated with key genes associated with terpenoid metabolic pathways and *PfERF106* potentially affects the synthesis of terpene floral substances by affecting key genes in the terpene metabolic pathway of *P. forbesii*.

To further verify the positive regulatory effect of *PfERF106* on the synthesis of terpenoids, this study found that the contents of key terpenoids were significantly increased by overexpression of *PfERF106*. This identification of floral gene function by both knockout and overexpression of function has also been accomplished in various plants, including *P. hybrida* [24] and *Lilium* 'Siberia' [61]. Notably, *PfERF106* plays a role in both homologous and heterologous plants. In contrast, Zhao et al. reported transient overexpression of *LcERF134* in *L. cubeba* increased monoterpene content, while its overexpression in tomatoes did not cause an increase in monoterpene content [62]. These contrasting results suggest that *LcERF134* is a specific transcription factor, while *PfERF106* is conserved in its control of the synthesis of terpenoid substances in *P. forbesii*. In addition, it was found that overexpression of *PfERF106* could advance the flowering stage of plants. This finding is

consistent with the findings of Xing et al., who found that constitutive expression of *CmERF110* from *Chrysanthemum morifolium* Ramat. in *A. thaliana* accelerated plant flowering [21]. Moreover, *A. thaliana AtERF110* is regulated by ethylene and participates in modulating the bolting time of flowers through protein phosphorylation [63]. Yan et al. performed transcriptome sequencing analysis on *Camellia oleifera* Abel. and thus identified *CoERF106*, a key pivotal gene closely associated with photoperiod-sensitive differential genes [64]. This finding suggests that *PfERF106* overexpression in *P. forbesii* potentially affects the expression level of photoperiodic pathway-related genes, thereby accelerating the flowering time of tobacco.

PfERF106 is involved in several terpenoid metabolic pathways

RNA sequencing (RNA-seq) is a reliable and versatile technology widely used in biosynthesis regulation studies of plant aromatic substances, including in *Prunus mume* Siebold & Zucc [65]. , *Hedychium coronarium* J [66]. , and *Cymbidium goeringii* Rchb. F [67].

In the present study, through transcriptome sequencing analysis of *PfERF106*-silenced plants and control plants, it was found that *PfERF106* affected the synthesis of various terpenoids, including both primary terpene metabolites, such as sterols, carotenoids, and hormones, and secondary or specialized terpene metabolites [68]. The present study focused on identifying downregulated DEGs that may be the downstream target genes of *PfERF106* in the MEP and MVA terpenoid synthesis pathways, including *DXS*, *HDR*, *GDPS*, *HMGR*, and *NES*, among others. *DXS* genes are divided into three types, each of which exhibits different expression patterns and functions in the specific development process and organs of plants in which they are involved [69]. Type I *DXS* genes include the *DXS1* (*CLA1*) gene from *A. thaliana*, which has been posited to have a major housekeeping function [70]. Type II *DXS* genes include *MtDXS2* from *Medicago truncatula* Gaertn. and *dxs2* from maize (*Z. mays*), whose expression is crucial to the accumulation of carotenoids in the process of plant mycorrhizalization [71, 72]. Type III *DXS* genes include *OsDXS3* in rice (*Oryza sativa* L.) and *PaDXS2A* and *PaDXS2B* in *Picea abies* L., which are mainly involved in defense responses and the generation of secondary metabolites [73, 74]. These results indicate that the *DXS* gene, as the first key enzyme gene in the MEP metabolic pathway, plays an important role in the synthesis of secondary metabolites. Notably, biological processes, such as photosystem and photosynthesis GO terms, were significantly enriched in the DEG pathways. This phenomenon was attributed to the regulation of the expression of *PfDXS2*, a key gene that encodes proteins localized to chloroplasts in the MEP metabolic pathway of *P. forbesii* [29], as determined by silencing the *PfERF106* gene, which affected the synthesis of volatile terpenes in flowers and plant photosynthesis.

One unigene annotated as the *HDR* gene was identified in the terpenoid backbone biosynthesis pathway. HDR, a key enzyme involved in the last step of the MEP pathway, synthesizes isopentenyl pyrophosphate (IPP) and dimethylallyl diphosphate (DMAPP) and plays an important role in isoprene biosynthesis [75]. Ma et al. found that overexpression of *AaHDR1* in *A. annua* significantly increased the contents of seven sesquiterpenoids, including artemisinin and artemisinin B, and eight monoterpenoids, including α-pinene, cineol, and sabinene [76]. Similarly, a unigene annotated as the *GDPS* gene was identified in the MEP pathway. The *PbGDPS* gene in *P. bellina* plays a crucial role in the release of monoterpene [77], suggesting that *PfGDPS* may also affect the release of monoterpene in *P. forbesii*. Beyond the MEP pathway, two unigenes annotated as *HMGR* and *AACT* were obtained from the MVA pathway. The two unigenes play important functions in terpenoid synthesis as key rate-limiting enzymes in the MVA metabolic pathway. For example, overexpression of *HMGR* in *N. tabacum* can lead to a 3- to 10-fold increase in total sterol level [78].

One *NES* gene in the monoterpenoid biosynthesis pathway was identified in this study. The *NES* annotation in the Swiss-Prot database was obtained from strawberry (*Fragaria* × *ananassa*) *FaNES1*. The *NES* gene encodes a bifunctional monoterpene and sesquiterpene synthase, which catalyzes the production of linalool by geranyl diphosphate (GDP) and nerolidol by farnesyl diphosphate (FDP). It is thus also called linalool/nerolidol synthase (*LIS/NES*) [79]. Overexpression of strawberry (*Fragaria* × *ananassa*) *FaNES1* in *A. thaliana* leaves produced free, hydroxylated, and glycosylated linalool derivatives [80, 81]. Similarly, Nagegowda et al. showed that the protein encoded by *AmNES/LIS-2* in *A. majus* was localized to plastids, but could catalyze the formation of linalool in plastids and nerolidol in cytoplasmic pathways at the same time, and sesquiterpene synthase activity was detected in white bodies [82]. Similarly, in *N. tabacum* and *S. tuberosum*, a small amount of the sesquiterpenoid precursor FDP was found in the plastid, and monoterpenoid precursor substances were found in the cytoplasm in metabolically engineered *A. thaliana* [80, 83, 84]. These results collectively suggest that there is a special relationship between linalool and nerolidol synthesis and the synthesis of downstream metabolites dependent on the content and proportion of precursor substances. The *NES1* gene identified in this study potentially participates in linalool synthesis, a key floral monoterpenoid in *P. forbesii*. The above studies indicate that the significantly

downregulated terpenoid synthesis genes identified in *PfERF106*-silenced plants are highly likely to participate in the regulation of floral terpenoids biosynthesis of *P. forbesii* as key downstream target genes of *PfERF106*. In the future, yeast one-hybrid and dual-luciferase assays will be further used to explore which *TPS* gene is regulated by this transcription factor and thus affects the change in terpene content.

In addition, key differentially expressed transcription factors, such as MYB and bHLH, were also identified in this study. MYB family genes participate in the biosynthesis of floral terpenoids. For example, Guo et al. identified the *Lilium* 'Siberia' transcription factors *LiMYB1*, *LiMYB305*, and *LiMYB330* as regulating terpenoid synthesis [61]. Abbas et al. found that five *HcMYB* genes in *H. coronarium* participated in the regulation of terpenoid and phenylpropane biosynthesis by activating genes involved in the biosynthesis of volatile compounds at the base of the bottom floral structure [85]. Xia et al. identified six *TwMYB* genes potentially involved in the regulation of terpenoid biosynthesis following a whole-genome analysis of the MYB gene family in *Tripterygium wilfordii* Hook. f [86]. Members of the bHLH family of transcription factors are also key regulators of plant-specific metabolites, such as the synthesis and regulation of terpenoid indole alkaloids (TIAs) in *C. roseus* [87]. In this study, a MYC transcription factor in the large bHLH transcription factor family was identified, suggesting the involvement of MYC family members in terpenoid synthesis in plants. For example, overexpression of the *LaMYC4* gene of lavender (*Lavandula angustifolia* Mill.) in *Arabidopsis thaliana* and tobacco (*N. tabacum*) increased the metabolism of sesquiterpenes, including caryophyllenes, in transgenic plants [88]. *CpMYC2* from *Chimonanthus praecox* L. is potentially involved in the positive regulation and biosynthesis of monoterpenes (linalool) and sesquiterpenes (β-caryophyllene) in transgenic plants [89]. These reports collectively suggest that the biosynthesis of linalool, a key floral component of *P. forbesii*, is potentially associated with MYC-class transcription factors. The TFs associated with the release of volatile compounds are strong candidates for future research.

Conclusion

In this study, *PfERF106*, an ethylene response factor with differential expression that consistently matched trends of floral components of terpenes in the aromatic plant *P. forbesii*, was identified and cloned. Bioinformatics and expression analyses were performed on the *PfERF106* gene to determine its spatiotemporal expression, response to exogenous ethylene treatment, and subcellular localization. Homologous instantaneous silencing and heterologous overexpression were used to verify the function of the *PfERF106* gene in the synthesis of floral terpenoids. The downstream target genes of *PfERF106* were screened and predicted by RNA sequencing, laying a molecular foundation for the future improvement of floral traits in *P. forbesii* through genetic engineering. The molecular data generated also provide high-quality genetic resources for aroma improvement in plants. Notably, the selected functional genes and transcription factors were not functionally verified. These genes, which are primarily associated with the release of volatile compounds, will be a key focus of future research.

Materials and methods

Plant materials and growth conditions

Primula forbesii was planted in the greenhouse facilities of the College of Landscape Architecture, Sichuan Agricultural University (30°42′N, 103°51′E) under a daytime temperature of 18 ± 2℃, nighttime temperature of 10 ± 2℃, and photocycle of 12/12 h (day/night). Petals from the bud stage, initial flowering stage, full flowering stage, and late flowering stage, as well as leaves, stem, and roots, were used as experimental materials for tissue-specific expression and flower development stage expression experiments. Samples were placed in a pre-cooled 1.5-mL centrifuge tube, immediately frozen in liquid nitrogen, and stored at -80℃ in an ultra-low temperature freezer prior to subsequent tests. The ethylene treatment experiment was applied following the method of Liu et al. [16]. Briefly, the flowers of *P. forbesii* in the full flowering stage were sampled and placed in a closed environment, incubated with ethylene at different concentrations (0, 5, 10, 15, and 20 μL/L) for 10 h, and then treated with ethylene at test concentrations for 0, 2, 4, 8, 12, and 24 h. The flower organs of 8 to 10 flowers were collected at each time point, immediately frozen in liquid nitrogen, and stored at -80℃ for easy RNA extraction. *Nicotiana benthamiana* Domin and *Nicotiana tabacum* cv. 'Samsun' grow under an average temperature of 24℃ and a photoperiod of 12/12 h (day/night).

Gene isolation and sequence comparison analysis

The full-length coding sequence (CDS) of *PfERF106* was amplified by PCR and sequenced after being cloned into a T vector. The primers that were used are listed in Supplementary Table 1 (Table S1). The NCBI database was used to predict the conserved domains of proteins encoded by *PfERF106*. The NLStradamus web tool (http://www.moseslab.csb.utoronto.ca/NLStradamus/) was used to predict nuclear localization signal of PfERF106. The sequences of ERF106 homologous proteins were downloaded from the GenBank. The ERF family protein sequences of *Arabidopsis thaliana* L. were downloaded from PlantTFDB 5.0.

Amino acid sequence alignment was performed using DNAMAN 8.0, followed by the construction of a phylogenetic tree using MEGA-X, with reference to the ERF family subgroup classification of *A. thaliana* [17].

RNA extraction, cDNA synthesis, and qRT-PCR

Total RNA was extracted using the RNAprep Pure Plant Plus Kit (TIANGEN, Beijing, China) following the manufacturer's instructions. The purity, concentration, and integrity of the RNA samples were detected using a NanoDrop spectrophotometer (Thermo Scientific, Waltham, MA, USA) and Agilent 2100 Bioanalyzer (Agilent Technologies, Santa Clara, CA, USA). The RNA samples were subsequently synthesized into cDNA using the Evo M-MLV reverse transcription premix kit (ACCURATE, Changsha, China). The qRT-PCR assay was performed using the SYBR Green Pro Taq HS premixed qPCR kit (ACCURATE, Changsha, China) on a Real-time quantitative PCR instrument (CFX Connect Bio-Rad, Hercules, CA, USA). Each qRT-PCR was replicated thrice, and the relative gene expression was analyzed using the $2^{-\Delta\Delta CT}$ method [90]. The qRT-PCR primers are listed in Table S2, Table S6, Table S7, and Table S8, respectively.

Subcellular localization

The target gene *PfERF106* was inserted into the *Eco*RI/*Spe*I site of p131-35 S-YFP using a seamless cloning method, followed by the transformation of the fusion plasmid into *Agrobacterium* strain GV3101. The primers for the construction of subcellular localization vectors are listed in Table S3. The *Agrobacterium* was prepared for injection by culturing it overnight, followed by centrifuge-mediated suspension in a solution containing 10 mmol/L $MgCl_2$, 10 mmol/L MES, and 100 μmol/L Acetosyringone. The *Agrobacterium* culture was allowed to stand for 3 h in the suspension solution at room temperature and was then injected into the leaves of *N. benthamiana* at the 4–5-leaf stage. The tobacco leaves were sampled 3 days after injection and observed under a confocal laser microscope (TCS SP8, Leica, Wetzlar, Germany). The excitation and emission wavelengths of yellow fluorescent protein (YFP) were 514 nm and 525–575 nm, while those of mCherry were 587 nm and 600–650 nm, respectively.

Transient silencing of *PfERF106* in *P. forbesii*

The *PfERF106*-silenced line of *P. forbesii* was obtained as described by Fu et al. using tobacco rattle virus (TRV) as a VIGS vector [91]. The primer sequences used for TRV vector construction are listed in Table S4. The infection solution prepared in advance (sterile water containing 10 mmol/L MES, 10 mmol/L $MgCl_2$, and 200 μmol/L Acetosyringone) was mixed with the *Agrobacterium* obtained after centrifugation to obtain a bacterial solution with a concentration of $OD_{600} = 1.0$. The bacterial solution containing TRV2-*PfPDS* and TRV2-*PfERF106* was left to stand for 3–4 h at room temperature. It was then mixed with the bacterial solution containing TRV1 at a ratio of 1:1 (*V*:*V*), and the mixture was subsequently slowly injected into the back of the leaves of *P. forbesii* until the leaves showed signs of impregnation. PCR-positive identification and expression level detection of transgenic strains were conducted after flowering (40 d post-infection). The primers used are listed in Table S5 and Table S2. Fresh petal samples (0.3 g) were placed in a 20-mL headspace bottle, followed by the addition of 5 μL of 0.5% ethyl caprate (anhydrous ethanol dissolved) as the internal standard. The volatile floral components were extracted following the method of Jia et al. [29] and determined by solid phase microextraction-gas chromatography-mass spectrometry (SPME-GC-MS). Each strain was measured thrice, and the relative content of each floral component was subsequently calculated using the method of Sheng et al. [92]. The mass fraction of each component was calculated using the following formula: Relative content of each component (μg/g, FW) = (peak area of each component/internal standard peak area) × (internal standard concentration × internal standard volume/sample mass). The key genes for terpenoid synthesis in *P. forbesii* were selected for expression detection, and the primer sequences are shown in Table S7.

Constitutive overexpression of *PfERF106* in tobacco

The transformation vector containing *PfERF106* (pCAMBIA2301-*PfERF106*) was transformed into *Agrobacterium* strain GV3101 using the leaf disk transformation method to overexpress *PfERF106* in *N. tabacum* constitutively. Leaves were infected with the *Agrobacterium* and kept in the dark for 24 h. Callus growth was subsequently induced in a medium supplemented with 50 mg/L kanamycin B and 400 mg/L cephalosporin. The callus was transferred to the screening and differentiation medium 30–45 d later to induce bud formation. The buds were then placed in Murashige and Skoog medium to induce root formation, after which the well-rooted seedlings were planted in soil in a greenhouse. The transformed plants were identified by PCR and analyzed by qRT-PCR to verify the relative expression of *PfERF106* in positive transgenic plants. The primers used are listed in Table S6. Fresh petal samples of wild-type tobacco and two independent transgenic tobacco lines with high *PfERF106* expression were harvested at the full flowering stage for volatile component analysis and quantification.

Transcriptome sequencing analysis

RNA was extracted from *PfERF106*-silenced transgenic lines and empty-vector control lines, synthesized into cDNA using the cDNA Synthesis kit following the manufacturer's protocol (Illumina, San Diego, CA, USA), and used to construct six libraries. The library quality was tested using the Agilent 2100 Bioanalyzer (Agilent, 2100) and Agilent High Sensitivity DNA Kit (Agilent, 5067 – 4626). The cDNA libraries were paired-end (PE) sequenced on a NovaSeq 6000 platform (Illumina). The raw sequence data were filtered using fastp (0.22.0) software to obtain high-quality sequences (Clean Reads). Unigene sequences were subsequently obtained by assembling the clean reads using Trinity (v2.15.1) software.

The obtained Unigenes were annotated for gene function using the NR (NCBI non-redundant protein sequences), GO (Gene Ontology), KEGG (Kyoto Encyclopedia of Genes and Genome), eggNOG (evolutionary genealogy of genes: Non-supervised Orthologous Groups), Swiss-Prot, and Pfam databases. RNA-seq by expectation maximization (RSEM v2.15) statistics were used to compare the reading values of each gene to the original expression level of each gene, while FPKM values were used to standardize the expression level. The DESeq (v1.38.3) software was used to analyze the differential gene expression based on fold change > 1.5 and p-value < 0.05 thresholds.

GO enrichment analysis was conducted with topGO (v2.50.0). The p-value was calculated using the hypergeometric distribution method (the criterion for significant enrichment was a p-value < 0.05 threshold) to identify the significantly enriched GO terms of the DEGs (among all, upregulated, and downregulated DEGs, respectively). This calculation was conducted to determine the main biological functions of the DEGs. The Cluster Profiler (v4.6.0) tool was used for the enrichment analysis of KEGG channels. Pathways exceeding a threshold of p-value < 0.05 were significantly enriched. Downregulated terpenoid synthetic genes were randomly selected for expression detection for RNA-seq data validation; the primer sequences used are shown in Table S8.

Supplementary Information

The online version contains supplementary material available at https://doi.org/10.1186/s12870-024-05567-7.

Supplementary Material 1.

Supplementary Material 2.

Supplementary Material 3.

Supplementary Material 4.

Acknowledgements
Not applicable.

Authors' contributions
Y J (Yin Jia), XC Y (Xiancai Yin), and HC Y (Hongchen Yang) designed experiments; XC Y (Xiancai Yin), KY D (Keying Ding) and YZ L (Yuanzhi Luo) performed experiments; XC Y (Xiancai Yin) and HC Y (Hongchen Yang) wrote the manuscript; WQ D (Wanqing Deng) and JW L (Jianwei Liao) analyzed data; YZ P (Yuanzhi Pan), BB J (Beibei Jiang), X Y (Xue Yong) and Y J (Yin Jia) reviewed and edited the original version of the manuscript. All authors read and approved the manuscript.

Funding
This work was supported by the National Natural Science Foundation of China (32001356).

Availability of data and materials
The datasets generated for this study are available in the NCBI Sequence Read Archive (SRA) under bioproject No. PRJNA1083092.

Declarations

Ethics approval and consent to participate
All our experiments have complied with relevant institutional, national, and international guidelines and legislation. Plant samples used in this study were cultivated by Professor Yin Jia from the College of Landscape Architecture, Sichuan Agricultural University, and have independent intellectual property rights. All methods and materials were in compliance with relevant institutional, national, and international guidelines and legislation. The plant materials don't include any wild species at risk of extinction. We comply with relevant institutional, national, and international guidelines and legislation for plant study.

Consent for publication
Not applicable.

Competing interests
The authors declare no competing interests.

Received: 25 May 2024 Accepted: 2 September 2024
Published online: 10 September 2024

References

1. Knudsen JT, Eriksson R, Gershenzon J, Stahl B. Diversity and distribution of floral scent. Bot Rev. 2006;72(1):1–120.
2. Xiao M, Zhang Y, Chen X, Lee EJ, Barber CJ, Chakrabarty R, et al. Transcriptome analysis based on next-generation sequencing of non-model plants producing specialized metabolites of biotechnological interest. J Biotechnol. 2013;166(3):122–34.
3. Dudareva N, Pichersky E. Metabolic engineering of plant volatiles. Curr Opin Biotechnol. 2008;19(2):181–9.
4. Dudareva N, Pichersky E. Biochemical and molecular genetic aspects of floral scents. Plant Physiol. 2000;122(3):627–33.
5. Gershenzon J, Dudareva N. The function of terpene natural products in the natural world. Nat Chem Biol. 2007;3(7):408–14.
6. Mahmoud SS, Croteau RB. Strategies for transgenic manipulation of monoterpene biosynthesis in plants. Trends Plant Sci. 2002;7(8):366–73.
7. Rodríguez-Concepción M, Boronat A. Elucidation of the methylerythritol phosphate pathway for isoprenoid biosynthesis in bacteria and plastids. A metabolic milestone achieved through genomics. Plant Physiol. 2002;130(3):1079–89.
8. Rohmer M. The discovery of a mevalonate-independent pathway for isoprenoid biosynthesis in bacteria, algae and higher plants. Nat Prod Rep. 1999;16(5):565–74.
9. Laule O, Fürholz A, Chang HS, Zhu T, Wang X, Heifetz PB, et al. Crosstalk between cytosolic and plastidial pathways of isoprenoid biosynthesis in *Arabidopsis thaliana*. Proc Natl Acad Sci U SA. 2003;100(11):6866–71.

10. Aharoni A, Galili G. Metabolic engineering of the plant primary-secondary metabolism interface. Curr Opin Biotechnol. 2011;22(2):239–44.
11. Hong GJ, Xue XY, Mao YB, Wang LJ, Chen XY. Arabidopsis MYC2 interacts with DELLA proteins in regulating sesquiterpene synthase gene expression. Plant Cell. 2012;24(6):2635–48.
12. Tian JP, Ma ZY, Zhao KG, Zhang J, Xiang L, Chen LQ. Transcriptomic and proteomic approaches to explore the differences in monoterpene and benzenoid biosynthesis between scented and unscented genotypes of wintersweet. Physiol Plant. 2019;166(2):478–93.
13. Ding W, Ouyang Q, Li Y, Shi T, Li L, Yang X, et al. Genome-wide investigation of WRKY transcription factors in sweet osmanthus and their potential regulation of aroma synthesis. Tree Physiol. 2020;40(4):557–72.
14. Zhou F, Sun TH, Zhao L, Pan XW, Lu S. The bZIP transcription factor *HY5* interacts with the promoter of the monoterpene synthase gene *QH6* in modulating its rhythmic expression. Front Plant Sci. 2015;6:304.
15. Allen MD, Yamasaki K, Ohme-Takagi M, Tateno M, Suzuki M. A novel mode of DNA recognition by a beta-sheet revealed by the solution structure of the GCC-box binding domain in complex with DNA. EMBO J. 1998;17(18):5484–96.
16. Liu J, Li J, Wang H, Fu Z, Liu J, Yu Y. Identification and expression analysis of ERF transcription factor genes in petunia during flower senescence and in response to hormone treatments. J Exp Bot. 2011;62(2):825–40.
17. Nakano T, Suzuki K, Fujimura T, Shinshi H. Genome-wide analysis of the ERF gene family in Arabidopsis and rice. Plant Physiol. 2006;140(2):411–32.
18. Okamuro JK, Caster B, Villarroel R, Van Montagu M, Jofuku KD. The AP2 domain of APETALA2 defines a large new family of DNA binding proteins in Arabidopsis. Proc Natl Acad Sci U S A. 1997;94(13):7076–81.
19. Riechmann JL, Meyerowitz EM. The AP2/EREBP family of plant transcription factors. Biol Chem. 1998;379(6):633–46.
20. Sakuma Y, Liu Q, Dubouzet JG, Abe H, Shinozaki K, Yamaguchi-Shinozaki K. DNA-binding specificity of the ERF/AP2 domain of Arabidopsis DREBs, transcription factors involved in dehydration- and cold-inducible gene expression. Biochem Biophys Res Commun. 2002;290(3):998–1009.
21. Xing X, Jiang J, Huang Y, Zhang Z, Song A, Ding L, et al. The constitutive expression of a Chrysanthemum ERF transcription factor influences flowering time in *Arabidopsis thaliana*. Mol Biotechnol. 2019;61(1):20–31.
22. Li S, Wang H, Li F, Chen Z, Li X, Zhu L, et al. The maize transcription factor *EREB58* mediates the jasmonate-induced production of sesquiterpene volatiles. Plant J. 2015;84(2):296–308.
23. Li X, Xu Y, Shen S, Yin X, Klee H, Zhang B, et al. Transcription factor *CitERF71* activates the terpene synthase gene *CitTPS16* involved in the synthesis of E-geraniol in sweet orange fruit. J Exp Bot. 2017;68(17):4929–38.
24. Liu F, Xiao Z, Yang L, Chen Q, Shao L, Liu J, et al. *PhERF6*, interacting with *EOBI*, negatively regulates fragrance biosynthesis in petunia flowers. New Phytol. 2017;215(4):1490–502.
25. Han Y, Wang H, Wang X, Li K, Dong M, Li Y, et al. Mechanism of floral scent production in Osmanthus fragrans and the production and regulation of its key floral constituents, β-ionone and linalool. Hortic Res. 2019;6:106.
26. Chuang YC, Hung YC, Tsai WC, Chen WH, Chen HH. *PbbHLH4* regulates floral monoterpene biosynthesis in Phalaenopsis orchids. J Exp Bot. 2018;69(18):4363–77.
27. Richards AJ. Primula. London: B.T. Batsford; 2012. p. 3–122.
28. Yin J, Hu D, Liu S, Jiang FX. Floral scent compounds of *Primula Forbesii*. Chem Nat Compd. 2017;53:968–70.
29. Jia Y, Yin X, Yang H, Xiang Y, Ding K, Pan Y, et al. Transcriptome analyses reveal the aroma terpeniods biosynthesis pathways of *Primula Forbesii* Franch. and the functional characterization of the *PfDXS2* gene. Int J Mol Sci. 2023;24(16): 12730.
30. Colinas M, Goossens A. Combinatorial transcriptional control of plant specialized metabolism. Trends Plant Sci. 2018;23(4):324–36.
31. Shoji T. The recruitment model of metabolic evolution: jasmonate-responsive transcription factors and a conceptual model for the evolution of metabolic pathways. Front Plant Sci. 2019;10:560.
32. Shoji T, Yuan L. ERF gene clusters: working together to regulate metabolism. Trends Plant Sci. 2021;26(1):23–32.
33. Dubos C, Stracke R, Grotewold E, Weisshaar B, Martin C, Lepiniec L. MYB transcription factors in Arabidopsis. Trends Plant Sci. 2010;15(10):573–81.
34. Rushton PJ, Somssich IE, Ringler P, Shen QJ. WRKY transcription factors. Trends Plant Sci. 2010;15(5):247–58.
35. Zhang F, Fu X, Lv Z, Lu X, Shen Q, Zhang L, et al. A basic leucine zipper transcription factor, *AabZIP1*, connects abscisic acid signaling with artemisinin biosynthesis in Artemisia annua. Mol Plant. 2015;8(1):163–75.
36. Menke FL, Champion A, Kijne JW, Memelink J. A novel jasmonate- and elicitor-responsive element in the periwinkle secondary metabolite biosynthetic gene Str interacts with a jasmonate- and elicitor-inducible AP2-domain transcription factor, ORCA2. EMBO J. 1999;18(16):4455–63.
37. Yu ZX, Li JX, Yang CQ, Hu WL, Wang LJ, Chen XY. The jasmonate-responsive AP2/ERF transcription factors *AaERF1* and *AaERF2* positively regulate artemisinin biosynthesis in Artemisia annua L. Mol Plant. 2012;5(2):353–65.
38. Berrocal-Lobo M, Molina A, Solano R. Constitutive expression of ETHYLENE-RESPONSE-FACTOR1 in Arabidopsis confers resistance to several necrotrophic fungi. Plant J. 2002;29(1):23–32.
39. Gu YQ, Wildermuth MC, Chakravarthy S, Loh YT, Yang C, He X, et al. Tomato transcription factors pti4, pti5, and pti6 activate defense responses when expressed in Arabidopsis. Plant Cell. 2002;14(4):817–31.
40. Tsubasa S, Takashi H. DNA-binding and transcriptional activation properties of tobacco NIC2-locus *ERF189* and related transcription factors. Plant Biotechnol. 2012;29(1):35–42.
41. Wang M, Gao M, Zhao Y, Chen Y, Wu L, Yin H, et al. *LcERF19*, an AP2/ERF transcription factor from Litsea cubeba, positively regulates geranial and neral biosynthesis. Hortic Res. 2022;9:uhac093.
42. Strader L, Weijers D, Wagner D. Plant transcription factors - being in the right place with the right company. Curr Opin Plant Biol. 2022;65: 102136.
43. Gu YQ, Yang C, Thara VK, Zhou J, Martin GB. Pti4 is induced by ethylene and salicylic acid, and its product is phosphorylated by the Pto kinase. Plant Cell. 2000;12(5):771–86.
44. Oñate-Sánchez L, Singh KB. Identification of Arabidopsis ethylene-responsive element binding factors with distinct induction kinetics after pathogen infection. Plant Physiol. 2002;128(4):1313–22.
45. Negre F, Kish CM, Boatright J, Underwood B, Shibuya K, Wagner C, et al. Regulation of methylbenzoate emission after pollination in snapdragon and petunia flowers. Plant Cell. 2003;15(12):2992–3006.
46. Schuurink RC, Haring MA, Clark DG. Regulation of volatile benzenoid biosynthesis in petunia flowers. Trends Plant Sci. 2006;11(1):20–5.
47. Underwood BA, Tieman DM, Shibuya K, Dexter RJ, Loucas HM, Simkin AJ, et al. Ethylene-regulated floral volatile synthesis in petunia corollas. Plant Physiol. 2005;138(1):255–66.
48. Sexton R, Stopford AP, Moodie WT, Porter AEA. Aroma production from cut sweet pea flowers (*Lathyrus odoratus*): the role of ethylene. Physiol Plant. 2005;124(3):381–9.
49. Millar AH, Carrie C, Pogson B, Whelan J. Exploring the function-location nexus: using multiple lines of evidence in defining the subcellular location of plant proteins. Plant Cell. 2009;21(6):1625–31.
50. Dhandapani S, Kim MJ, Chin HJ, Leong SH, Jang IC. Identification and functional characterization of tissue-specific terpene synthases in *Stevia rebaudiana*. Int J Mol Sci. 2020;21(22):8566.
51. Lu R, Martin-Hernandez AM, Peart JR, Malcuit I, Baulcombe DC. Virus-induced gene silencing in plants. Methods. 2003;30(4):296–303.
52. Lee SY, Kang B, Venkatesh J, Lee JH, Lee S, Kim JM, et al. Development of virus-induced genome editing methods in Solanaceous crops. Hortic Res. 2024;11(1):uhad233.
53. Wang Y, Guo Y, Guo S, Qi L, Li B, Jiang L, et al. RNA interference-based exogenous double-stranded RNAs confer resistance to Rhizoctonia Solani AG-3 on Nicotiana tabacum. Pest Manag Sci. 2024;80(4):2170–8.
54. Broderick SR, Chapin LJ, Jones ML. Virus-induced gene silencing for functional analysis of flower traits in Petunia. Methods Mol Biol. 2020;2172:199–222.
55. Xu Y, Ji X, Xu Z, Yuan Y, Chen X, Kong D, et al. Transcriptome profiling reveals a Petunia transcription factor, *PhCOL4*, contributing to antiviral RNA silencing. Front Plant Sci. 2022;13: 876428.
56. Zhang Y, Ji A, Xu Z, Luo H, Song J. The AP2/ERF transcription factor SmERF128 positively regulates diterpenoid biosynthesis in *Salvia miltiorrhiza*. Plant Mol Biol. 2019;100(1–2):83–93.
57. Bai Z, Li W, Jia Y, Yue Z, Jiao J, Huang W, et al. The ethylene response factor *SmERF6* co-regulates the transcription of *SmCPS1* and *SmKSL1* and is involved in tanshinone biosynthesis in *Salvia miltiorrhiza* hairy roots. Planta. 2018;248(1):243–55.

58. Zhu K, Sun Q, Chen H, Mei X, Lu S, Ye J, et al. Ethylene activation of carotenoid biosynthesis by a novel transcription factor *CsERF061*. J Exp Bot. 2021;72(8):3137–54.
59. Wei C, Li M, Cao X, Jin Z, Zhang C, Xu M, et al. Linalool synthesis related *PpTPS1* and *PpTPS3* are activated by transcription factor *PpERF61* whose expression is associated with DNA methylation during peach fruit ripening. Plant Sci. 2022;317:111200.
60. Wan L, Huo J, Huang Q, Ji X, Song L, Zhang Z, et al. Genetics and metabolic responses of Artemisia annua L to the lake of phosphorus under the sparingly soluble phosphorus fertilizer: evidence from transcriptomics analysis. Funct Integr Genom. 2024;24(1):26.
61. Guo Y, Guo Z, Zhong J, Liang Y, Feng Y, Zhang P, et al. Positive regulatory role of R2R3 MYBs in terpene biosynthesis in Lilium'Siberia'. Hortic Plant J. 2023;9(5):1024–38.
62. Zhao Y, Wang M, Chen Y, Gao M, Wu L, Wang Y. *LcERF134* increases the production of monoterpenes by activating the terpene biosynthesis pathway in *Litsea cubeba*. Int J Biol Macromol. 2023;232: 123378.
63. Zhu L, Liu D, Li Y, Li N. Functional phosphoproteomic analysis reveals that a serine-62-phosphorylated isoform of ethylene response factor110 is involved in Arabidopsis bolting. Plant Physiol. 2013;161(2):904–17.
64. Yan J, He J, Li J, Ren S, Wang Y, Zhou J, et al. Analysis of *Camellia Oleifera* transcriptome reveals key pathways and hub genes involved during different photoperiods. BMC Plant Biol. 2022;22(1):435.
65. Xiujun W, Zhenqi S, Yujing T, Kaifeng M, Qingwei L. Comparative transcriptome analysis linked to key volatiles reveals molecular mechanisms of aroma compound biosynthesis in *Prunus mume*. BMC Plant Biol. 2022;22(1):395.
66. Yue Y, Yu R, Fan Y. Transcriptome profiling provides new insights into the formation of floral scent in *Hedychium coronarium*. BMC Genomics. 2015;16(1):470.
67. Ramya M, Park PH, Chuang YC, Kwon OK, An HR, Park PM, et al. RNA sequencing analysis of *Cymbidium Goeringii* identifies floral scent biosynthesis related genes. BMC Plant Biol. 2019;19(1):337.
68. Nagegowda DAJFL. Plant volatile terpenoid metabolism: biosynthetic genes, transcriptional regulation and subcellular compartmentation. FEBS Lett. 2010;584(14):2965–73.
69. Cordoba E, Porta H, Arroyo A, San Román C, Medina L, Rodríguez-Concepción M, et al. Functional characterization of the three genes encoding 1-deoxy-D-xylulose 5-phosphate synthase in maize. J Exp Bot. 2011;62(6):2023–38.
70. Kim BR, Kim SU, Chang YJ. Differential expression of three 1-deoxy-D: -xylulose-5-phosphate synthase genes in rice. Biotechnol Lett. 2005;27(14):997–1001.
71. Floss DS, Hause B, Lange PR, Küster H, Strack D, Walter MH. Knock-down of the MEP pathway isogene 1-deoxy-D-xylulose 5-phosphate synthase 2 inhibits formation of arbuscular mycorrhiza-induced apocarotenoids, and abolishes normal expression of mycorrhiza-specific plant marker genes. Plant J. 2008;56(1):86–100.
72. Walter MH, Hans J, Strack D. Two distantly related genes encoding 1-deoxy-d-xylulose 5-phosphate synthases: differential regulation in shoots and apocarotenoid-accumulating mycorrhizal roots. Plant J. 2002;31(3):243–54.
73. Okada A, Shimizu T, Okada K, Kuzuyama T, Koga J, Shibuya N, et al. Elicitor induced activation of the methylerythritol phosphate pathway toward phytoalexins biosynthesis in rice. Plant Mol Biol. 2007;65(1–2):177–87.
74. Phillips MA, Walter MH, Ralph SG, Dabrowska P, Luck K, Urós EM, et al. Functional identification and differential expression of 1-deoxy-D-xylulose 5-phosphate synthase in induced terpenoid resin formation of Norway spruce (*Picea abies*). Plant Mol Biol. 2007;65(3):243–57.
75. Cheng Q, Tong Y, Wang Z, Su P, Gao W, Huang L. Molecular cloning and functional identification of a cDNA encoding 4-hydroxy-3-methylbut-2-enyl diphosphate reductase from *Tripterygium Wilfordii*. Acta Pharm Sinica B. 2017;7(2):208–14.
76. Ma D, Li G, Zhu Y, Xie DY. Overexpression and suppression of *Artemisia annua* 4-hydroxy-3-methylbut-2-enyl diphosphate reductase 1 gene (AaHDR1) differentially regulate artemisinin and terpenoid biosynthesis. Front Plant Sci. 2017;8:77.
77. Chuang YC, Hung YC, Hsu CY, Yeh CM, Mitsuda N, Ohme-Takagi M, et al. A dual repeat *cis*-element determines expression of GERANYL DIPHOSPHATE SYNTHASE for monoterpene production in Phalaenopsis orchids. Front Plant Sci. 2018;9:765.
78. Dai Z, Cui G, Zhou SF, Zhang X, Huang L. Cloning and characterization of a novel 3-hydroxy-3-methylglutaryl coenzyme a reductase gene from *Salvia miltiorrhiza* involved in diterpenoid tanshinone accumulation. J Plant Physiol. 2011;168(2):148–57.
79. Aharoni A, Jongsma MA, Bouwmeester HJ. Volatile science? Metabolic engineering of terpenoids in plants. Trends Plant Sci. 2005;10(12):594–602.
80. Aharoni A, Giri AP, Deuerlein S, Griepink F, de Kogel WJ, Verstappen FW. Terpenoid metabolism in wild-type and transgenic Arabidopsis plants. Plant Cell. 2003;15(12):2866–84.
81. Aharoni A, Giri AP, Verstappen FW, Bertea CM, Sevenier R, Sun Z. Gain and loss of fruit flavor compounds produced by wild and cultivated strawberry species. Plant Cell. 2004;16(11):3110–31.
82. Nagegowda DA, Gutensohn M, Wilkerson CG, Dudareva N. Two nearly identical terpene synthases catalyze the formation of nerolidol and linalool in snapdragon flowers. Plant J. 2008;55(2):224–39.
83. Aharoni A, Jongsma MA, Kim TY, Ri MB, Giri AP, Verstappen FWA, et al. Metabolic engineering of terpenoid biosynthesis in plants. Phytochem Rev. 2006;5(1):49–58.
84. Wu S, Schalk M, Clark A, Miles RB, Coates R, Chappell J. Redirection of cytosolic or plastidic isoprenoid precursors elevates terpene production in plants. Nat Biotechnol. 2006;24(11):1441–7.
85. Abbas F, Ke Y, Zhou Y, Yu Y, Waseem M, Ashraf U, et al. Genome-wide analysis reveals the potential role of MYB transcription factors in floral scent formation in *Hedychium coronarium*. Front Plant Sci. 2021;12:623742.
86. Xia M, Tu L, Liu Y, Jiang Z, Wu X, Gao W, et al. Genome-wide analysis of MYB family genes in *Tripterygium Wilfordii* and their potential roles in terpenoid biosynthesis. Plant Direct. 2022;6(7):e424.
87. Singh SK, Patra B, Paul P, Liu Y, Pattanaik S, Yuan L. BHLH IRIDOID SYNTHESIS 3 is a member of a bHLH gene cluster regulating terpenoid indole alkaloid biosynthesis in *Catharanthus roseus*. Plant Direct. 2021;5(1):e00305.
88. Dong Y, Zhang W, Li J, Wang D, Bai H, Li H, et al. The transcription factor *LaMYC4* from lavender regulates volatile terpenoid biosynthesis. BMC Plant Biol. 2022;22(1):289.
89. Aslam MZ, Lin X, Li X, Yang N, Chen L. Molecular cloning and functional characterization of *CpMYC2* and *CpBHLH13* transcription factors from Wintersweet (*Chimonanthus praecox* L). Plants (Basel). 2020;9(6):785.
90. Livak KJ, Schmittgen TD. Analysis of relative gene expression data using real-time quantitative PCR and the 2(-Delta Delta C(T)) method. Methods. 2001;25(4):402–8.
91. Fu ST, Si WJ, Liu Y, Cheng TR, Wang J, Zhang QX, et al. Establishing tobacco rattle virus-mediated gene silencing system for *Primula Forbesii*. Biotechnol Bull. 2022;38(04):295–302 (in Chinese).
92. Sheng L, Zeng Y, Wei T, Zhu M, Fang X, Yuan X, et al. Cloning and functional verification of genes related to 2-phenylethanol biosynthesis in *Rosa rugosa*. Genes. 2018;9(12):576.

Publisher's note